Ozonvertikalverteilungen und stratosphärische Säulen von NO2, OClO, und BrO aus GOME und SCIAMACHY Nadirsatellitendaten: Optimierung der Datenprodukte und wissenschaftliche Studien zur Chemie und Dynamik der unteren Stratosphäre (GOMSTRAT)

Vertical ozone distributions and stratospheric columns of NO2, OClO, and BrO from GOME and SCIAMACHY nadir satellite data: Data product optimization and scientific studies of the lower stratospheric dynamics and chemistry (GOMSTRAT)

Endbericht/Final Report

Projektdauer: 1.4.2001-31.10.2004
BMBF-Förderkennzeichen 07ATF42
Projektträger: GSF-UKF

Autoren:
M. Weber, K. Bramstedt, J.P. Burrows, M. Coldewey-Egbers, S. Dhomse, L.N. Lamsal, A. Richter, B.-M. Sinnhuber, S. Tellmann, und V. Rozanov

Projektleiter: Dr. Mark Weber (weber@uni-bremen.de)

April 2005

Kontakt:
Dr. Mark Weber
Institut für Umweltphysik (IUP)
Universität Bremen FB1
Postfach 330 440
D-28334 Bremen

Tel. 0421/218-2362
Fax 0421/218-4555
email: weber@uni-bremen.de
www.iup.uni-bremen.de

Berichtsblatt

1. ISBN oder ISSN	2. Berichtsart Endbericht	

3a. Titel des Berichts

Ozonvertikalverteilungen und stratosphärische Säulen von NO2, OClO, und BrO aus GOME und SCIAMACHY Nadirsatellitendaten: Optimierung der Datenprodukte und wissenschaftliche Studien zur Chemie und Dynamik der unteren Stratosphäre (GOMSTRAT)

3b. Titel der Publikation

4a. Autoren des Berichts (Name, Vorname(n)) M. Weber, K. Bramstedt, J.P. Burrows, M. Coldewey-Egbers, S. Dhomse, L.N. Lamsal, A. Richter, B.-M. Sinnhuber, S. Tellmann, and V. Rozanov	5. Abschlussdatum des Vorhabens 31. Oktober 2005
4b. Autoren der Publikation (Name, Vorname(n))	6. Veröffentlichungsdatum Juli 2005
	7. Form der Publikation

8. Durchführende Institution(en) (Name, Adresse) Universität Bremen FB1 Institut für Umweltphysik Postfach 330 440 D-28334 Bremen Deutschland	9. Ber. Nr. Durchführende Institution
	10. Förderkennzeichen *) BMBF-Förderkennzeichen 07ATF42
	11a. Seitenzahl Bericht
	11b. Seitenzahl Publikation
13. Fördernde Institution (Name, Adresse) Bundesministerium für Bildung und Forschung (BMBF) 53170 Bonn	12. Literaturangaben
	14. Tabellen
	15. Abbildungen

16. Zusätzliche Angaben

17. Vorgelegt bei (Titel, Ort, Datum)

18. Kurzfassung

Gesamtziel des Projektes ist die Ableitung von qualitativ hochwertigen Langzeit-Messreihen von Ozonprofilen und stratosphärischen Säulen von O3, NO2, BrO und OClO aus den Nadir UV/VIS Spektralmessungen der Satelliteninstrumente GOME und SCIAMACHY. Die erzeugten Datensätze bilden für die statistische Auswertung der chemischen und dynamischen Prozesse in der Stratosphäre eine wichtige Grundlage, insbesondere auch im Zusammenhang mit möglichen Klimaänderungen. Notwendige Voraussetzung für die wissenschaftlichen Studien ist die Entwicklung beschleunigter und verbesserter Algorithmen in der Profil- und Säulenauswertung. Bei der Bestimmung der stratosphärischen Säulen von NO2 und BrO sind bestehende Verfahren zur Trennung von troposphärischen und stratosphärischen Anteilen an der gemessenen Gesamtsäule exemplarisch am Beispiel von GOME NO2 Messungen untersucht worden.

19. Schlagwörter

Ozon, Atmosphärenchemie, atmosphärischer Transport, Stratosphäre, Spurengase, Inversionsverfahren, Satellitenmessungen

20. Verlag	21. Preis

---

*) Auf das Förderkennzeichen des BMBF soll auch in der Veröffentlichung hingewiesen werden.

BMBF-Vordr. 3831/03.99

Document Control Sheet

1. ISBN or ISSN	2. Type of Report Final Report

3a. Report Title
Vertical ozone distributions and stratospheric columns of NO2, OCIO, and BrO from GOME and SCIAMACHY nadir satellite data: Data product optimisation and scientific studies of the lower stratospheric dynamics and chemistry (GOMSTRAT)

3b. Title of Publication

4a. Author(s) of the Report (Family Name, First Name(s)) M. Weber, K. Bramstedt, J.P. Burrows, M. Coldewey-Egbers, S. Dhomse, L.N. Lamsal, A. Richter, B.-M. Sinnhuber, S. Tellmann, and V. Rozanov	5.End of Project 31 October 2004
4b. Author(s) of the Publication (Family Name, First Name(s))	6. Publication Date July 2005
	7. Form of Publication

8. Performing Organization(s) (Name, Address) University of Bremen FB1 Institute of Environmental Physics PO Box 330 440 D-28334 Bremen Germany	9. Originator's Report No.
	10. Reference No., BMBF-Förderkennzeichen 07ATF42
	11a. No. of Pages Report
	11b. No. of Pages Publication
13. Sponsoring Agency (Name, Address) Bundesministerium für Bildung und Forschung (BMBF) D-53170 Bonn Germany	12. No. of References
	14. No. of Tables
	15. No. of Figures

16. Supplementary Notes

17. Presented at (Title, Place, Date)

18. Abstract
The main goal of this project is to derive high quality trace gas distributions, ozone profiles and stratospheric O3 NO2, BrO, and OCO columns, from longterm global nadir UV/visible spectral data measured by GOME and SCIAMACHY. These data sets were used in a statistical analysis of chemical and dynamical processes in the lower stratosphere that are relevant to possible future climate change. A prerequisite for successful scientific studies using global satellite data is the development of improved and accelerated algorithms to retrieve ozone profiles and trace gas columns. Different methods to derive BrO, NO2, and ozone stratospheric columns from methods that separate tropospheric and stratospheric contributions from the measured total column were demonstrated using NO2 from GOME as an example.

19. Keywords
ozone, atmospheric chemistry, atmospheric transport, stratosphere, trace constituent, satellite retrieval

20. Publisher	21. Price

BMBF-Vordr. 3832/03.99

Contents

1 Vorblatt

1.1 Verwertungsplan

Im Rahmen unseres Projekts wurden zwei verbesserte Methoden zur Bestimmung von Ozonprofilen und -säulen aus GOME Satellitendaten in Nadir-Beobachtungsgeometrie erstellt. Damit ist es nun möglich den gesamten Zeitraum der globalen GOME Messungen von 1995 bis 2003 auszuwerten. Für das Gesamtozon sind Daten bereits auf unserer Homepage verfügbar (www.iup.uni-bremen.de/gome/wfdoas). Die GOME Ozonprofilauswertung hat sehr grosse Fortschritte gemacht durch eine stark verbesserte und global anwendbare Kalibrationskorrektur, die insbesondere die fortschreitenden Verschlechterung der optischen Eigenschaften korrigiert. Jedoch war der Aufwand für die Optimierung grösser als ursprünglich geplant, so dass die Auswertung für den achtjährigen Zeitraum im Rahmen dieses Projekts nicht mehr vollzogen werden kann. Es wird angestrebt durch eine weitere Finanzierung diesen Datensatz für die wissenschaftliche Nutzung bereitzustellen.

Mehrere Verfahren zur Trennung von stratosphärischen und troposphärischen Teilsäulen der schwachen Absorber wurden am Beispiel von NO_2 vorgestellt und für die GOME Auswertung angewendet. Diese Trennung ist wichtig für Prozessstudien und die Interpretation der Spurengasdaten. Die entwickelten Algorithmen und Verfahren sind für die Anwendung auf SCIAMACHY (seit 2002), OMI (seit 2004), und den drei GOME2/METOP Instrumenten (ab 2006) ebenso geeignet. Mit den verschiedenen Satelliteninstrumenten und den verbesserten Algorithmen ist eine wesentliche Grundlage für die Homogenisierung der verschiedenen Langzeitdatensätze auf Zeitskalen von Dekaden gewährleistet.

Die im Rahmen dieser Studie aktualisierte Ozonprofilklimatologie dient auf der einen Seite als verbesserte Constraints im Ozonretrievalverfahren. Darüberhinaus ist sie auch sehr wertvoll für die Initialisierung von Klima- und Chemietransportmodellen, die zur Untersuchung von atmosphärischen Prozessen und für die Prognose der zukünftigen Entwicklung der Atmosphäre im Zusammenhang mit dem Klimawandel eingesetzt werden.

Desweiteren wurden in dieser Studie Untersuchungen zur Ozonvariabilität anhand der GOME Daten durchgeführt, die die enge Kopplung zwischen der Dynamik (Transport) und Chemie in mittleren bis hohen Breiten aufzeigten. Für die Vorhersage der weiteren Entwicklung der Ozonschicht ist neben der erwarteten Abnahme des stratosphärischen Chlorgehalts noch ungewiss ob sich die Ozonschicht wie erwartet wieder erholen wird oder ob durch Änderungen in der stratosphärischen Zirkulation aufgrund von Klimaveränderungen die Erholung entweder verlangsamt oder sogar beschleunigen wird. Hier werden in den nächsten Jahre interessante Ergebnisse zu erwarten sein auch mit Hilfe der jetzt verfügbaren Satellitendatensätzen, die lange Zeiträume abdecken.

Insgesamt zehn begutachtete Artikel in Fachzeitschriften, eine Masterarbeit und eine Doktorarbeit sind aus dieser Studie hervorgegangen. Drei weitere Doktorarbeiten werden im Laufe des Jahres fertiggestellt und weitere Publikationen im Zusammenhang mit dieser Studie werden vorbereitet.

1.2 Aufzählung der wichtigsten wissenschaftlichen Ergebnissen/ Erfolgskontrollbericht

Die wichtigsten Ergebnisse dieser Studie sind im folgenden einzeln aufgelistet.

Weber et al. *Universität Bremen*

- Die Auswertung der Ozonprofile aus Nadirspektraldaten von GOME wurde mit Hilfe verschiedener Kalibrationskorrekturen stark verbessert. Mit Hilfe von mit GOME kollokierten HALOE Ozonprofilen sind Korrekturfunktionen für die radiometrische Eichung der GOME Spektren mit Hilfe von Strahlungstransportrechungen bestimmt worden. Diese Korrektur berücksichtigt auch die Veränderung der optischen Eigenschaften des Instrumentes über die gesamte Lebenszeit von 1996 bis 2003. Dies verbessert die Ozonprofilauswertung der GOME Daten über den gesamten Zeitraum bei nahezu gleichbleibender Datenqualität. Vielversprechende erste Ergebnisse zur Ableitung von troposphärischen Ozon aus den Nadirprofilen von GOME wurden erzielt.

- Die Entwicklung des neuen Ozonsäulenalgorithmus WFDOAS (Weighting Function DOAS) für GOME wurde erfolgreich eingeführt und Daten der Jahre 1995 bis 2003 wurden ausgewertet und sind im Netz verfügbar (www.iup.uni - bremen.de/gome/wfdoas). Erste Anwendung auf SCIAMACHY sind vielversprechend. Der neue Ozonsäulenalgorithmus wurde durch Vergleiche mit global verteilten Bodenmessungen ausführlich validiert. Die Resultate zeigen eine Übereinstimmung unter einem 1%. Dies ist wichtig für die Nutzung der Daten für Langzeittrends.

- Eine aktualisierte Ozonprofilklimatologie bestehend aus mehr als zehn Jahren umfassenden Messungen von Satelliten (SAGE, POAM) und Ozonsonden wurde nach geographischen und atmosphärendynamischen Kriterien zusammengestellt. Diese Klimatologie dient vorwiegend als Nebenbedingung (*constraints*), z.B. in der Ozonprofilauswertung, oder als a-priori Information, z.B. bei der WFDOAS Ozonsäulenauswertung. Die Ergebnisse sind im Netz unter www .iup.uni-bremen.de/gome/o3climatology verfügbar.

- Erste Ergebnisse zum Verfahren der Trennung von troposphärischen und stratosphärischen Anteilen an der gemessenen Gesamtsäulendichten von schwachen Absorbern, hier am Beispiel von NO_2 von GOME, erzielt. Diese Ansätze können bei den neuen Generation von Nadirsoundern SCIAMACHY (seit 2002), OMI (seit 2004) und GOME2 (ab 2006) angewendet werden.

- Mit Hilfe der GOME und SCIAMACHY Daten wurden Untersuchungen zum Einfluss dynamischer (Transport) und chemischer Prozesse auf die hemisphärische Ozonverteilung im späten Winter und Frühjahr gemacht. Dabei zeigt sich, dass der Transport von Ozon als Teil der Meridional- oder Residualzirkulation und die Chemie (z.B. durch Chloraktivierung) sehr stark gekoppelt sind. Diese enge Kopplung wurde exemplarisch im sogenannten Fall der Ozonlochanomalie in der Antarktis im Winter 2002 untersucht. Neben den Änderungen im stratosphärischen Chlorgehalt in Folge des Montreal Protokols spielen klimarelevante Prozesse (z.B. durch Erderwärmung), die die grossräumige Zirkulation beeinflussen, eine wichtige Rolle in der zukünftigen Entwicklung der Ozonschicht.

Es sind bisher insgesamt neun begutachtete (*peer reviewed*) Publikationen aus dem GOMSTRAT Projekt hervorgegangen (siehe Abschnitt 3). Darüberhinaus ist jeweils eine Masterarbeit und eine Dissertation hervorgegangen.

1.3   Vergleich des Vorhabenstands mit der ursprünglichen Planung

Arbeits- und Zeitplanung

Arbeits- und Zeitplanung sind im Soll bis auf die globale Ozonprofilauswertung der GOME Daten für den gesamten Zeitraum 1996 bis 2003 mit der neuen Version 6.

Ausgabenplanung
keine Änderung

1.4 Änderung der Vorhabensziele

keine Änderung

1.5 Relevanz der Ergebnisse von dritter Seite für das Vorhaben

nicht bekannt

1.6 Erfindungen und Lizenzen

keine

1.7 Mittelverbrauch

Personaleinsatz
Lok Lamsal (BATIIa/2, 1.2.2002-31.3.2004)
Sandip Dhomse (BATIIa/2, 1.4.2002-31.3.2004)
Lars Hild (BATIIa/2, 1.1.2002-21.3.2002, 1.8.2002-31.12.2002)
Hilke Oeljen (BATIIa, 1.11.2002-31.12.2002)
Dr. Mark Weber (BATIIa, 1.1.2004-30.6.2004)

Anschaffungen (Posten 850)
PC und Zubehör (2 Stück)
RAID Massenspeicher mit Backup Software

1.8 Unterschrift

Bremen, den 1.7.2005

(Mark Weber)

2 Kurzzusammenfassung

2.1 Abstract (German)

Gesamtziel des Projektes ist die Ableitung von qualitativ hochwertigen Langzeit-Meßreihen von Ozon-profilen und stratosphärischen Säulen von O_3, NO_2, BrO und OClO aus den Nadir UV/VIS Spektralmessungen der Satelliteninstrumente GOME und SCIAMACHY. Die erzeugten Datensätze bilden für die statistische Auswertung der chemischen und dynamischen Prozesse in der Stratosphäre eine wichtige Grundlage, insbesondere auch im Zusammenhang mit möglichen Klimaänderungen.

Notwendige Voraussetzung für die wissenschaftlichen Studien ist die Entwicklung beschleunigter und verbesserter Algorithmen in der Profil- und Säulenauswertung. Bei der Bestimmung der stratosphärischen Säulen von NO_2 und BrO sind bestehende Verfahren zur Trennung von troposphärischen und stratosphärischen Anteilen an der gemessenen Gesamtsäule exemplarisch am Beispiel von GOME NO_2 Messungen untersucht worden.

2.2 Abstract (English)

The main goal of this project is to derive high quality trace gas dristributions, ozone profiles and strato-spheric O_3, NO_2, BrO, and OClO columns, from longterm global nadir UV/visible spectral data measured by GOME and SCIAMACHY. These data sets were used in a statistical analysis of chemical and dynamical processes in the lower stratosphere that are relevant to possible future climate change.

A prerequisite for successful scientific studies using global satellite data is the development of improved and accelerated algorithms to retrieve ozone profiles and trace gas columns. Different methods to derive BrO, NO_2, and ozone stratospheric columns from methods that separate tropospheric and stratospheric contributions from the measured total column were demonstrated using NO_2 from GOME as an example.

3 Wissenschaftlicher Bericht/ Scientific Report (in English)

3.1 Introduction

The Global Ozone Monitoring Experiment (GOME) is the first European space-borne atmospheric chemistry experiment for global long-term trend measurements [Burrows et al., 1999]. GOME was successfully launched aboard the ERS-2 satellite in 1995 and global spectral data have been recorded continuously up to now. However, in June 2003 the on-board tape recorder failed so that the coverage of GOME observations has been reduced to the European Atlantic sector where the space craft is in direct contact with ground stations. The GOME instrument has been succeeded by SCIAMACHY aboard ENVISAT that was launched in 2002 [Bovensmann et al., 1999]. This instrument has an extended spectral range including near infrared and additional scanning modes (limb and occultation in addition to nadir sounding).

The large spectral coverage of GOME (and SCIAMACHY) from 240 nm to the near infrared and moderate high spectral resolution of 0.2–0.4 nm permits the retrieval of many key trace gas species that are important for chemical and transport processes in the atmosphere. With the so called DOAS method (Differential Optical Absorption Spectroscopy) vertical column densities (total columns) of several trace gases can be derived in the nadir viewing mode [Burrows et al., 1999].

Routine operational column retrieval is done for ozone and NO_2. Other trace gases such as BrO, OClO, SO_2 (volcanic emission) and formaldehyde (bio mass burning) have been detected with GOME [Burrows et al., 1999]. The nadir retrieval of column amounts can be continued with only minor modifications with SCIAMACHY [Bovensmann et al., 1999].

Dynamical (transport) and chemical processes in the atmosphere are strongly altitude dependent and, therefore, require vertical profile information of trace gases for scientific investigations. A special focus of this project is to further improve ozone profile retrieval from nadir observations that is based upon an advanced optimal estimation inversion scheme that we call Full Retrieval Method FURM [de Beek et al., 1996, 1997, Hoogen et al., 1999b,a]. Other trace gases than ozone can only be retrieved as total column amounts. The conversion of slant column amounts derived using DOAS (Differential Optical Absorption Spectroscopy) into vertical columns are done by calculating airmass factor from radiative transfer calculations. Specific methods can be used to separate tropospheric and stratospheric columns and they are investigated as part of this project [Burrows et al., 1999, Richter et al., 1998b].

This report is divided into four parts. In Section 3.2 the optimized ozone profile retrieval scheme is presented that contains an elaborate calibration correction to account for instrument degradation over the lifetime of GOME. An important aspect of the optimal estimation procedure used in the ozone profiling is the selection of proper constraints. The new ozone profile shape climatology that has been created as part of this study (Section 3.3) can be used as additional constraints to stabilize the retrieval. This climatology can also serve as a-priori information needed in the new improved total ozone algorithm based upon the weighting function differential optical absorption spectroscopy technique (WFDOAS). The WFDOAS scheme is described in Section 3.4. Several methods to separate tropospheric and stratospheric columns from measured total column of minor absorbers are presented in 3.5.

The various retrieval techniques can be applied to other UV/visible space borne spectrometers such as SCIAMACHY (launch in 2002), OMI (launch in 2004) and the three GOME2 aboard Metop 1, 2, and 3

(first launch in 2006). In Section 3.6 the close coupling of dynamical (transport) and chemical processes on ozone is investigated as an example of the usefulness of long-term satellite data sets that have been developed as part of this study.

3.2 Nadir ozone profiling of GOME with an improved global calibration scheme

Ozone vertical distributions can be retrieved from GOME UV/VIS spectra by application of the FURM (FUll Retrieval method) algorithm which is based upon an advanced optimal estimation approach including the optimal estimation scheme and the eigenvector method from Kozlov [de Beek et al., 1997, Hoogen et al., 1999b,a]. This algorithm is applied to the spectral region between 290 nm and 340 nm. Over the years several improvements particularly with regard to the radiometric calibration of the GOME radiance and solar irradiance measurements have continously increased the accuracy of the GOME ozone profiles. In FURM V5 an empirical correction using two separate sets of Chebyshev polynomials were fitted to Channel 1 (below 314 nm) and Channel 2 (above 314 nm) to account for jumps in the spectral data between the channels. Nadir profiling was limited to wavelengths larger than 290 nm because of unusual large residuals observed at lower wavelengths. The lower boundary of 290 nm reduces the altitude coverage to about 35 km altitude and below. In the short wavelength region subtraction of a polynomial as a first order correction can correlate with broad band ozone features and can lead to larger errors in the upper stratospheric profiles. As part of this project two major improvements towards FURM version 6 have been applied: 1) extension of short-wave region down to 275 nm, and 2) a correction for the optical degradation of GOME with time.

3.2.1 Additive and multiplicative calibration correction

The increasing calibration problems of GOME with decreasing wavelengths are mainly caused by the optical degradation of the instrument due to the harmful UV radiation in space. There have been some shortcomings due to the empirical nature of the calibration correction as obvious in Fig. 1. As a consequence application of earlier versions of FURM (Version 5.0) were restricted to the spectral range above 290 nm that led to a very weak retrieval sensitivity to ozone above 35 km.

First investigations of profile retrieval using wavelengths below 290 nm showed that the GOME reflectance (ratio of nadir earthshine spectrum over solar irradiance) are filled-in near the peaks of solar Fraunhofer lines when compared to modeled reflectances (see Fig. 1). This could not be explained by rotational Raman scattering [Vountas et al., 1998]. This effect is more likely an error in the dark current and/or stray light correction. This normally is a constant offset that, however, leads to larger (relative) errors in cases of low reflectances like in the regions of Fraunhofer structures. The additive correction, therefore, is apparently proportional to the inverse of the solar irradiance and it is used as an additional fitting term to match the modeled reflectance to the measured one.

An approach has been developed that assumes that the true atmospheric intensity $\frac{R_{atm}}{Irr_{atm}}$ calibrated by the standard calibration function (SCF) of the GOME data processor is still disturbed by multiplicative errors $m(\lambda)$ and additive errors a as follows.

$$\frac{R_{meas}}{Irr_{meas}} = SCF(\lambda)(1 + m(\lambda))\frac{R_{atm} + a(\lambda)}{Irr_{atm}}. \tag{1}$$

R_{meas} is the GOME nadir radiance spectrum as a function of wavelength λ, Irr_{meas} the solar irradiance spectrum. R_{atm} and Irr_{atm} are the true atmospheric radiative quantities. It is assumed that additive errors may be caused by errors in the dark current or instrumental stray-light measurements and are, therefore,
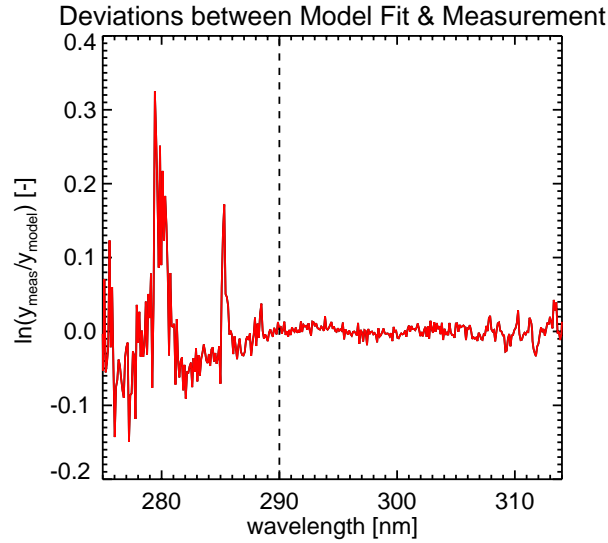
Figure 1: *Residual between GOME measured intensity and FURM model intensity. Dashed line: Start wavelength of FURM standard version (V5.0).*

expected to be proportional to the inverse irradiance of GOME, e.g.

$$a \sim \frac{SCF(\lambda)}{Irr_{atm}}. \tag{2}$$

A comparison between GOME measured intensities and FURM model intensities shows that the large filling-in of Fraunhofer lines which is obviously not explainable with rotational Raman-scattering can be to a large extent be corrected by fitting this inverse irradiance (Fig. 2).

The FURM retrieval version 5 allows for broadband multiplicative errors $m(\lambda)$ by fitting Chebyshev polynomials, but additive errors $a(\lambda)$ have not been taken into account. There were two separate set of Chebyshev polynomials fitted in Channel 1 (290-314 nm) and 2 (314-340 nm) [Hoogen et al., 1999b,a]. By extending the fitting window down to 275 nm a third set of Chebyshev polynomials were fitted initially. It turned out that the fitted polynomials showed strong correlation with ozone absorption that has little differential structures. For this reason, the additive (dark current) and multiplicative (polynomial correction) are first applied in a pre-fit to the 275-300 nm fitting window including the first ozone eigenvector. The difference between the modeled and observed reflectance then forms the multiplicative term in Channel 1 (275-300 nm) for the full retrieval that still fits two separate sets of Chebyshev polynomials to two windows, 300-314 nm and 314-340 nm, respectively. The ozone profile obtained from the pre-fit is used as a-priori information in the optimal estimation retrieval [Tellmann, 2005]

The comparison of this new retrieval scheme and FURM Version 5 with two ozone sonde flights from Hohenpeissenberg in South Germany demonstrates the significant improvement as shown in Fig. 3. The agreement between the ozone peak altitudes of GOME and sondes is striking. Particularly in the tropics where the ozone maximum is shifted to higher altitudes the inclusion of shorter wavelengths is essential for an accurate ozone profile retrieval [Tellmann et al., 2004].
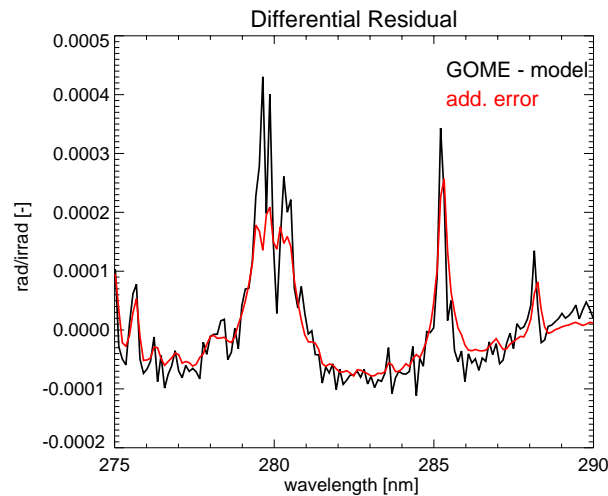
Figure 2: *Difference between FURM and GOME reflectivities (black) after subtraction of a polynomial and fit of additive error (red).*

3.2.2 Time dependent optical degradation correction

In the middle and high latitudes where the ozone maximum is shifted to lower altitudes, the differential absorption structures of ozone below 300 nm are quite weak and can therefore result in strong correlations between ozone and the broadband calibration corrections of FURM in this spectral range. The requirement of a modified broadband calibration correction led to a long term investigation of residuals between GOME measured spectra and model spectra calculated with HALOE ozone data (*HALogen Occultation Experiment*) using a radiative transfer model for a large number of collocations between GOME and HALOE. The annual mean residuals are shown in Fig. 4 for selected years. The residuals are fairly stable for a given year and these residual spectra are fitted to the GOME data to improve the calibration correction.

In FURM Version 6.0 the calibration correction based upon collocated HALOE profiles has been included. In order to demonstrate the improvement in the upper stratospheric retrieval, the sum of rows of the averaging kernel matrix has been calculated. It can be interpreted as the information content in the measurements. The new version (FURM 6.0) reveals an increased sensitivity to upper stratospheric ozone up to 50 km altitude in comparison with former results (FURM V5.0). Values larger than one denote an enhanced sensitivity to the measurement (see Fig. 5). As an example for the re-processing of the GOME data with this new version, a comparison between the two retrieval versions (V5 and V6) and collocated SAGE II (*Stratospheric Aerosol and Gas Experiment II*) is shown for the year 2003 as displayed in Fig. 6. In 2003 the optical degradation of the GOME instrument was already quite advanced after eight years of space operations. The typical underestimation of upper stratospheric ozone which can be seen in former results of the retrieval algorithm (FURM V5.0) has now been corrected.
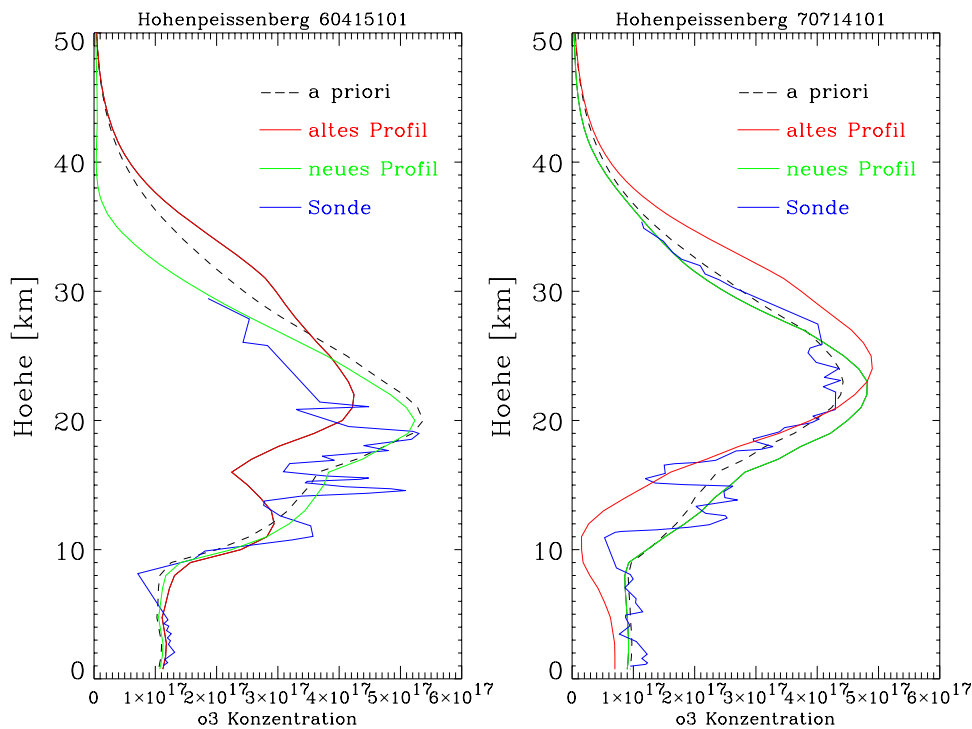
Figure 3: *Comparison between FURM GOME profiles with collocated ozone sonde data from Hohenpeissenberg* $(47.5^o N, 11.0^o E)$. *Shown are results from FURM V5 (altes Profil) and the new FURM results using additive and multiplicative correction factors (neues Profil). Also shown are the a-priori ozone profiles that are used as constraints in the optimal estimation retrieval.*

3.2.3 Tropospheric column retrieval

An improved stratospheric profile retrieval gives us also the capability to investigate tropospheric columns. The tropospheric ozone absorption structures, mainly observed at larger wavelengths in GOME channel 2, are very weak with respect to the stratospheric ozone and are not correctly fitted during the profile fitting. A differential spectral fit in Channel 2 is performed after the profile fit to account for remaining tropospheric ozone absorption structures in the fit residuals. The tropospheric columns calculated from integrating the profiles up to the thermal tropopause as derived from ECMWF met analyses are compared to collocated sonde results in Hohenpeissenberg in Fig. 7. Both results from the optimal estimation (red) and the two part retrieval including the differential fitting (blue) are shown in this scatter plot. Shown are here the differences between GOME retrieval and sonde results as well as the difference between a-priori climatology from Fortuin and Kelder [1998] and sondes. It can be clearly seen that the differential spectral fit reduces the correlation between tropospheric retrieval and a-priori climatology in comparison with the optimal estimation retrieval. This is very promising for the derivation of tropospheric information from nadir space soundings.
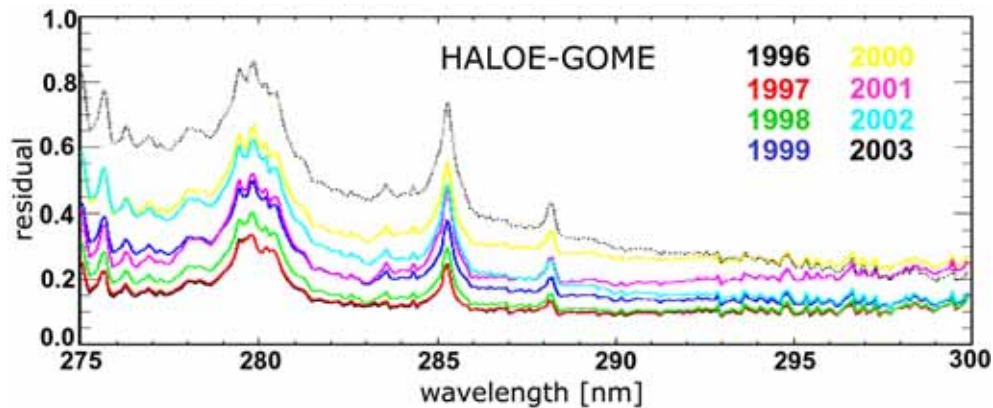
Figure 4: *Mean deviations between GOME measured spectra and model spectra calculated with collocated HALOE data. Shown are the annual mean deviations between 1996 and 2003.*
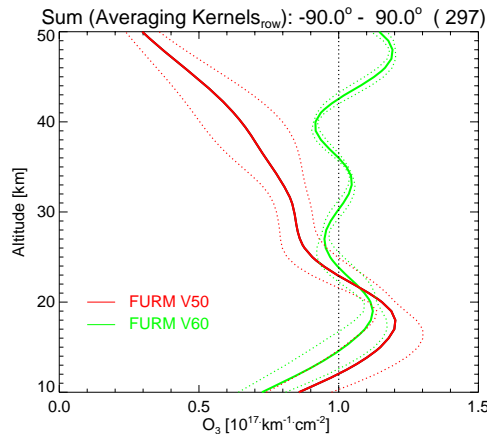
Figure 5: *Sum of rows of the averaging kernel matrix as an indicator for the sensitivity of the optimal estimation retrieval to the measurement.*

3.2.4   Conclusion and Outlook

The new global calibration approach enables us to extend the wavelength range to shorter wavelengths and enhances, therefore, the stratospheric information content of the retrieval. From comparisons with collocated HALOE ozone data, a degradation correction function was derived that is included in the optimal estimation retrieval at wavelengths below 290 nm. This empirical calibration correction enables us to extend the meaningful profile retrieval to year 2003 despite significant optical degradation of the GOME spectrometer. The improved stratospheric profile fit in turn also enhances the sensitivity in the tropospheric ozone column retrieval, derived from a differential spectral fit in GOME channel 2 (above 320 nm) following the stratospheric profile retrieval.
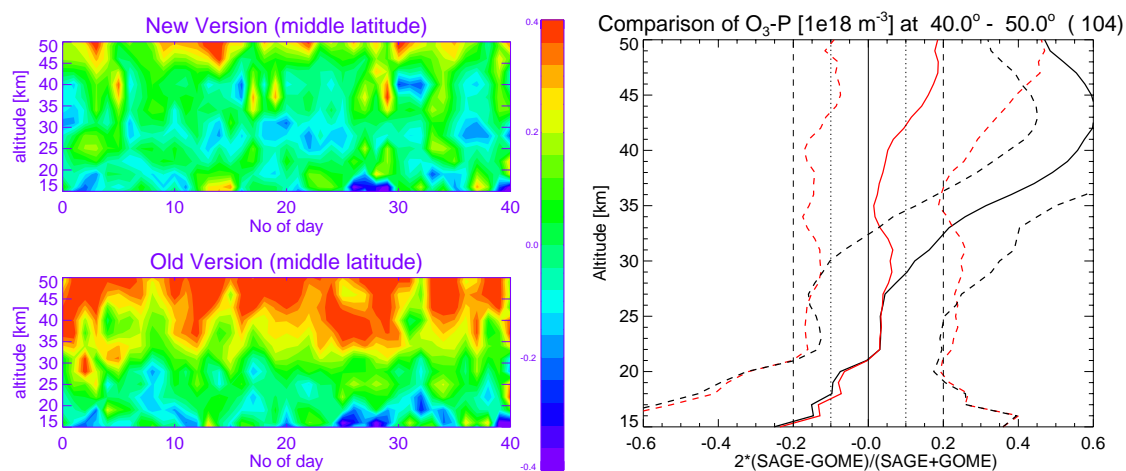
Figure 6: *Left panels: Relative deviations between FURM retrieval and SAGE measurement for 1997 in northern middle latitudes. Upper left panel shows new version (FURM V6.0) and lower left panel the older version (FURM V5.0). Right panel: Mean relative deviations between FURM and SAGE profiles in middle latitudes during 2003 (red: new version, black: old version). Dashed lines are the 1σ standard deviation of mean difference.*
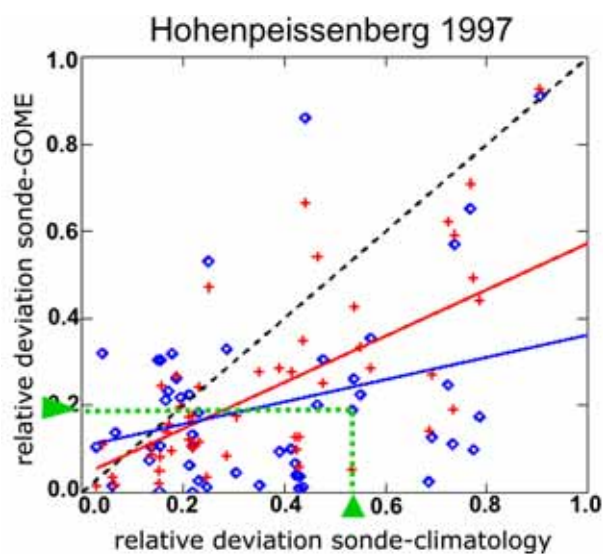
Figure 7: *Comparison of GOME tropospheric columns as well as a priori climatological values with collocated sonde results from Hohenpeissenberg in 1997. Red crosses are the results from the advanced optimal estimation method (FURM V6) and blue diamonds are from the two step fitting where in the second step a differential fitting in Channel 2 followed the FURM retrieval. A-priori climatological values were used as constraints in the optimal estimation and differential fitting. The green arrows shows one example where the differential fitting improved and reduced the difference of the GOME results with respect to the sonde (y-axis) as compared to the sonde-climatology difference (x-axis).*

3.3 New global ozone profile climatology

3.3.1 IUP ozone and temperature profile climatology

An updated and atmospheric dynamics oriented global climatology of ozone profiles has been derived from ozonesonde and satellite observations [Lamsal et al., 2004]. The climatology, which uses total ozone to parameterize the profile shape, provides improved a priori information for ozone profile retrieval from satellite measurements using optimal estimation. It can be also used to correct for the profile shape error in total ozone retrieval. Sonde data were selected from 1990-2000 and 1988-1999 period for SAGE II excluding two years of SAGE II V6.1 data influenced by the Pinatubo eruption in 1991. In addition, POAM III V3 data covering the polar region and SHADOZ ozonesonde data in the tropics were included. The ozone profile data were binned in steps of 30 DU of total ozone, 30° wide zonal bands, and into a six-month season (winter/spring and summer/fall) in middle and high latitude [Lamsal et al., 2004]. No seasonal distinction is needed in the low latitude region (30°S to 30°N). Mean and standard deviation profiles for each ozone class are combined from satellites and sondes with a transition region in the range of 20-26 km to merge both data sets.

Temperature data from sonde, SAGE II collocated NMC met analysis, and POAM III collocated UKMO met abnalyis, the latter used in their ozone retrieval, respectively, have been binned and averaged in the same manner as the ozone profiles so that for each mean ozone profile a matching temperature profile was derived. Corresponding ozone and temperature profiles help accounting for the temperature dependence of the ozone absorption cross-sections in the retrieval process. It was also found that there is a quite strong correlation between ozone and temperature for various altitudes [Lamsal et al., 2004, Steinbrecht et al., 2003]. Figures 8 and 9 show the 1σ variability expressed in percentage of the mean temperature and mean ozone profiles, respectively, for given total ozone values in various local regions and seasons.

3.3.2 Impact of ozone climatology on nadir ozone profiling

Good agreement between collocated sonde profiles from Hohenpeissenberg (48°N, 11°N) and GOME ozone profiles, retrieved using FURM V6 and using this climatology (mean ozone and temperature profiles and ozone standard deviations as constraints), was found. Figure 10 summarizes the comparison between GOME vertical ozone profiles derived with the zonal monthly mean ozone climatology from Fortuin and Kelder [1998], on one hand, and our new climatology, on the other, with results from collocated ozone sondes launched in Hohenpeissenberg (50 profiles) during 1997. It demonstrates the large improvements achieved by using this new climatology, particularly in the lowermost stratosphere and tropopause region.

The mean profile of the new climatology agrees to better than 10% with the mean sonde profile with a root mean square of the mean relative deviation being less than 20% in most cases except in the tropopause. The difference between mean of the zonal monthly mean climatology and averaged sonde results from Hohenpeissenberg in the tropopause region is up to 40% and a factor of four higher compared to result from our climatology. The retrieved mean GOME profile shows a significant improvement in the troposphere by using our updated climatology presented here. Despite the improvement of the GOME retrieval using the new climatology a positive bias in the GOME-sonde mean differences in the lowermost stratosphere remains. This can be explained by the asymmetric averaging kernels that smooth
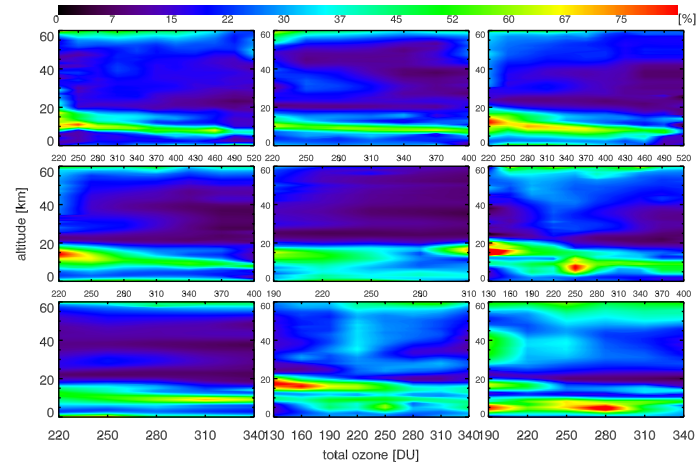
Figure 8: *One-sigma variability of ozone (in %) as a function of altitude and total ozone. Variability is highest in the lowermost stratosphere and upper troposphere. The plots are ordered from first row left to last row right as follows: NH polar winter/spring, NH polar summer/fall, NH midlatitude winter/spring, (second row) NH midlatitude summer/fall, tropics, SH midlatitude winter/spring, (third row) SH midlatitude summer/fall, SH polar winter/spring and SH polar summer/fall. From Lamsal et al. [2004]*
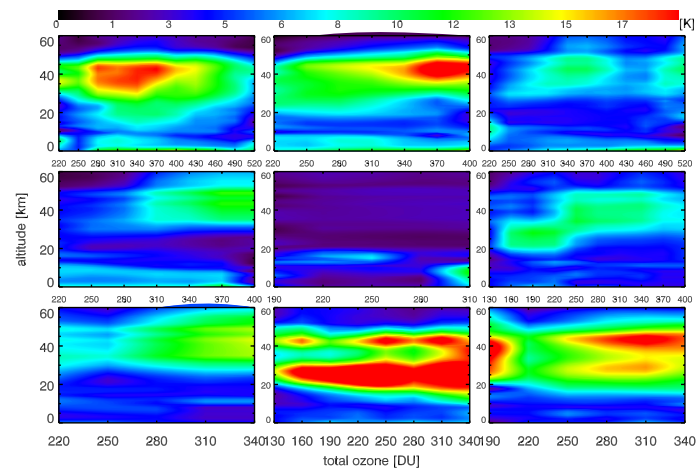
Figure 9: *One-sigma variability of temperature (in %) as a function of altitude and total ozone. As in the case of ozone, variability is highest in the lowermost stratosphere and upper troposphere. The plots are ordered from first row left to last row right as follows: NH polar winter/spring, NH polar summer/fall, NH midlatitude winter/spring, (second row) NH midlatitude summer/fall, tropics, SH midlatitude winter/spring, (third row) SH midlatitude summer/fall, SH polar winter/spring and SH polar summer/fall. From Lamsal et al. [2004]*
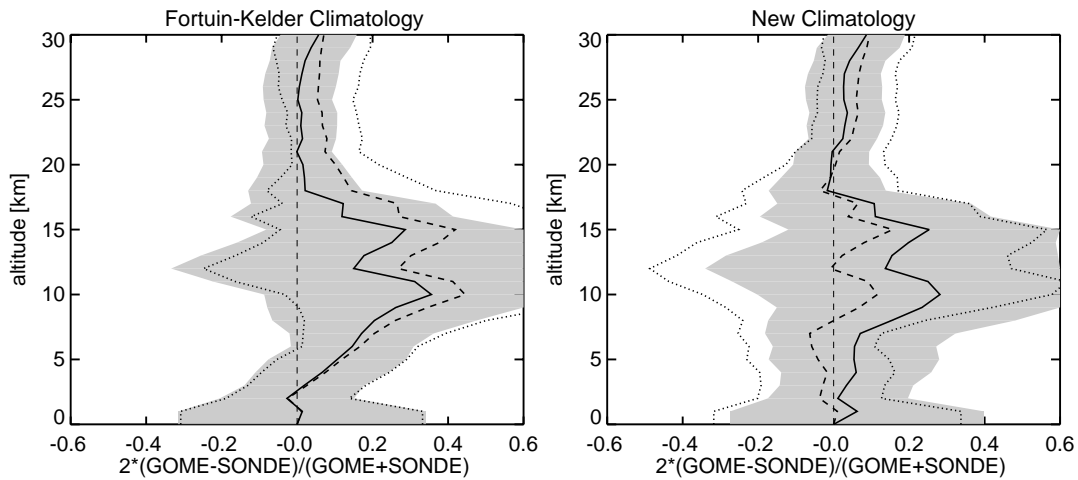
Figure 10: *Mean relative deviation between retrieved GOME and ozone sonde profiles (solid line) and between climatological and ozone sonde profiles (dashed line), respectively, in Hohenpeissenberg in 1997 (50 profiles). The profiles were retrieved using zonal monthly mean climatology (left panel) and our climatology (right panel) as constraints in the optimal estimation retrieval. The shaded region shows the root mean square of mean relative deviation for the retrieval and the dotted line the 1σ standard deviation of both climatologies. From Lamsal et al. [2004]*

the GOME profiles. In the lowermost stratosphere contribution from the ozone maximum increases the retrieved ozone down to the tropopause region [Hoogen et al., 1999b, Meijer et al., 2003].

3.3.3 Conclusion

A new ozone profile climatology has been developed that is based upon updated satellite and sonde data extending up to early 2000s. Total ozone has been used as a dynamical proxy to classify the profiles. matching the total ozone classification, corresponding mean temperature profiles has been constructed. The new climatology is of importance for ozone retrieval that need a-priori information as additional constraints. It is also valuable for initializing climate and chemistry-transport models.

3.4   Weighting function DOAS for total ozone retrieval from GOME

GOME is the first European experiment dedicated to global ozone measurements [Burrows et al., 1999]. The current operational total ozone retrieval GOME Data Processor Version 3.0 (GDP V3.0) shows some shortcomings when comparing satellite data with ground-based data. A seasonal cycle and variations with solar zenith angle can be observed when compared to ground data [GDP V3 VALREPORT]. The standard Differential Optical Absorption Spectroscopy (DOAS) method is used in the operational retrieval and slant columns derived from a spectral fit are converted into vertical columns using air mass factors at a single wavelength. This approach assumes that the absorber is weak and the atmosphere optically thin. Ozone in the Huggins band, however, shows significant absorption so that this basic assumption is violated.

A more generalized approach, called weighting Function DOAS (WFDOAS) has been introduced for total ozone retrieval. It has been first demonstrated to be applicable to trace gas column retrieval in the near infrared region of SCIAMACHY [Buchwitz, 2000, Buchwitz et al., 2000]. A direct retrieval of vertical ozone amounts is possible as the slant path wavelength modulation is taken into account [Coldewey-Egbers et al., 2004, 2005].

3.4.1   Theory and retrieval scheme

In the WFDOAS algorithm the measured atmospheric optical depth is approximated by a Taylor expansion around a reference intensity plus a low-order polynomial. The total column information is obtained only from differential trace gas structures as in case of standard DOAS and the polynomial accounts for all broadband contributions from surface albedo and aerosol.

Additional fit parameters are the Ring effect, the under-sampling correction, both treated as effective absorbers similar to the approach used in standard DOAS, and a (ozone) temperature shift [Coldewey-Egbers et al., 2005]. Slant column fitting is also applied to the minor absorbers NO_2 and BrO. All fit parameters are derived using a linear least squares minimization. A large set of reference spectra has been constructed that includes nearly all possible atmospheric conditions. The radiance spectra and weighting functions were calculated as a function of total ozone including profile shape, solar zenith angle, line-of-sight, relative azimuth angle, and bottom-of-atmosphere altitude and albedo using the multiple scattering SCIATRAN radiative transfer model in the pseudo-spherical approximation [Rozanov et al., 1998].

Ozone and temperature profiles are taken from TOMS V7 climatology [Wellemeyer et al., 1997] which contains different profile shapes for three latitude belts (low, middle and high) as a function of the total ozone column varying from 125-575 DU in mid and high latitudes and from 225-475 DU in low latitudes. In a future version update. the new atmospheric dynamics oriented climatology that has been developed as part of this study will be included. Solar zenith angle varies from $15°$ to $92°$, line-of-sight varies from $-34.5°$ to $+34.5°$, and the range for the relative azimuth angle is defined by a given combination of both parameters. Altitude of the boundary in the lower atmosphere varies from 0 to 12 km, and surface albedo from 0.02 to 0.98. Both parameters are considered effective parameters that take into account partial cloud cover in the GOME scene.

For ozone retrieval with WFDOAS the following data and information are required: Calibrated GOME level 1 radiance and solar spectrum from the same day, a-priori values for total ozone (initial guess),
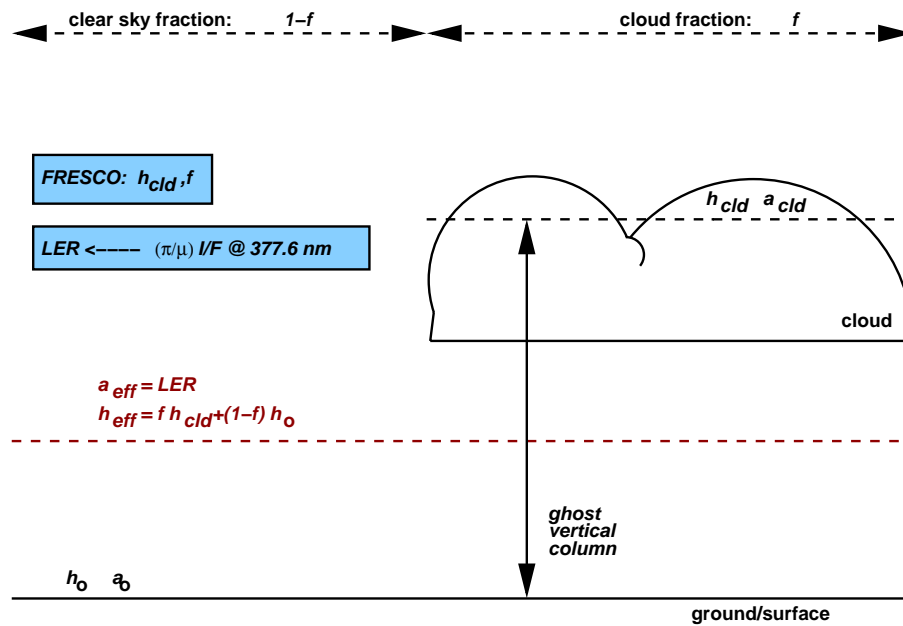
Figure 11: *Schematics of cloud retrieval (cloud fraction f and cloud-top-height h_{cld}) and the determination of effective height h_{eff} and ozone ghost vertical column GVC (see text for details). Other parameters are cloud top albedo (a_{cld}, here assumed to be 0.8), surface albedo (a_o), effective scene albedo (a_{eff}), and effective scene height or bottom-of-atmosphere (h_{eff}). From Coldewey-Egbers et al. [2005]*

effective altitude, and effective albedo. Effective altitude is obtained from FRESCO (Fast Retrieval Scheme for Clouds from the Oxygen A-Band, Koelemeijer et al. [2001]). Cloud top pressure and cloud fraction are derived from the oxygen transmittance assuming a high reflecting boundary representing the cloud top. Surface albedo is taken from minimum spectral reflectances derived from a five year GOME data record [Koelemeijer et al., 2003]. The effective height is the sum of the ground altitude and the retrieved cloud top height weighted by the fractional cloud cover (see Fig. 11).

The Lambertian equivalent reflectivity (LER, Herman and Celarier [1997]) defines the effective albedo and is obtained from GOME sun-normalized radiances at 377.6 nm, where variations with respect to the Ring effect are small and can be easily corrected for. A look-up-table of radiances as a function of solar zenith angle, line-of-sight, relative azimuth angle, ground altitude, and surface albedo has been pre-calculated using SCIATRAN and the LER are retrieved by finding the best match between calculated and measured TOA reflectance by inverse search in the multidimensional table.

The spectral window 326.8-335.0 nm is used in the ozone fitting procedure. After the iteration stops, the ghost vertical column (GVC), that is hidden below the (partial) cloud, is determined from an ozone climatology, multiplied by the cloud fraction, and then added to the retrieved column to obtain the final total ozone amount. In Fig. 11 the cloud retrieval and GVC determination is schematically described.
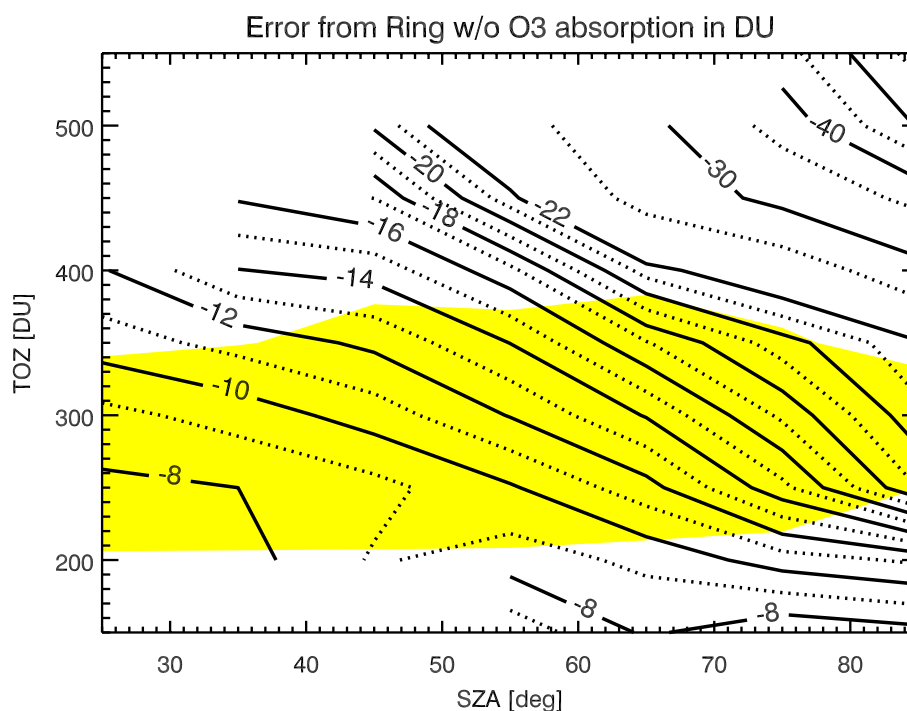
Figure 12: *Differences in total ozone between retrievals with Ring effect calculated without and with ozone absorption as a function of retrieved total ozone (TOZ) and solar zenith angle (SZA). The shading indicates the cumulative 90% case probabilities of a given SZA and total ozone combination from the analysis of 113 GOME orbits (about 205,000 individual retrievals). From Coldewey-Egbers et al. [2005]*

3.4.2 Treatment of the Ring effect

Satellite instruments such as GOME and TOMS observe the filling-in of solar Fraunhofer lines in the scattered light. Rotational Raman Scattering on air molecules is the most dominant contribution and has to be accounted for when retrieving trace gas columns. The WFDOAS algorithm uses the so-called Ring spectrum, which is the optical depth difference of intensities with and without the Ring effect [Joiner and Barthia, 1995, Vountas et al., 1998]. This spectrum is treated as an effective absorber in DOAS. Not only air molecules but also ozone as well as clouds modulate the scattered intensity (strong absorber) and has a non-negligible contribution to the molecular filling-in [Joiner and Bhartia, 1995, de Beek et al., 2001]. Figure 12 shows differences in total ozone retrieved from 113 GOME orbits distributed over eight selected days in 1997 by using two different Ring implementations, one including ozone absorption (and TOMS V7 profile shape climatology) and the second without ozone absorption. Differences of up to 10% at high total ozone above 500 DU can be observed. With respect to Ring calculations using a fixed atmosphere (with ozone typically near 300 DU) the error can still reach -5% above 500 DU [Coldewey-Egbers et al., 2005].

3.4.3   Global error budget

This section summarizes the most important error sources that contribute to the overall error of the retrieved ozone column. Propagating forward all errors that were identified, one arrives at a precision of the WFDOAS total ozone retrieval on the order of 3%. The error increases at solar zenith angles above 80°to at least 5%. The largest contribution comes from the a-priori errors associated with the use of climatology and simplifying assumptions made in the derivation of effective parameters. They may reach 2% below 80°SZA. Non-absorbing aerosols that are not accounted for in the radiative transfer are to first order corrected by including the effective albedo in the fitting. However, in the presence of absorbing aerosols (volcanic or urban type), ozone columns may be underestimated by 1% or more. Other potential errors to total ozone retrieval from GOME type instruments can be found in Coldewey-Egbers et al. [2005] and de Beek et al. [2004].

3.4.4   Validation of WFDOAS

Station data from the World Ozone and Ultraviolet Radiation Data Center (WOUDC) and Network for the Detection of Stratospheric Changes (NDSC) were selected for the global comparison [Weber et al., 2005]. They comprise of Dobson, Brewer and SAOZ spectrometers, but Dobsons are in majority. The collocation radius was set to less than 300 km between satellite and the correlative data and both are from the same day. At mid-latitudes (30°-60°) excellent agreement between WFDOAS and WOUDC data has been reached (see Fig. 13). Seasonal variation in the observed differences are generally below ±0.5%, while GDP V3 and TOMS V8 show larger annual variations on the order of ±1.5% and ±1%, respectively. No significant solar zenith angle (SZA) dependence is observed in the WFDOAS-station differences. GOME V3 underestimates (1 to 2%) in the tropics, while WFDOAS agrees to within 1%.

At polar latitudes WFDOAS differences increase on average to 2 to 5% at high solar zenith angles particularly for those stations which are near/inside the polar vortex. Under ozone hole condition WFDOAS differences can be as high as 6% to 8% (see Fig. 14). A strong positive bias is also observed with GOME V3 and TOMS V8 with respect to ground data at high solar zenith angle in polar region. This observed satellite-station bias may come from (1) stratospheric ozone temperature correction that is not accounted for in the retrieval technique of Dobson/Brewer measurements but in the GOME retrieval, (2) enhanced stray light problem associated with both satellite and ground measurements due to low light levels, and (3) other sources originating from instrumental differences and differences in retrieval wavelengths. Nevertheless, the accuracy of the WFDOAS results are to within the uncertainty of the ground-based measurements at high latitudes, see for instance results from the TOMS3-F campaign at Fairbanks [Staehelin et al., 2003], where improved stray-light and ozone temperature correction lead to differences of +3 to +4% in the ground data compared to the WMO-GAW standard retrieval.

Figure 15 shows the monthly mean differences between WFDOAS and collocated Dobson (both direct sun and zenith-sky) from Lauder (45°S) for the period 1996-2003. Particularly striking is the long-term stability of the GOME retrieval, despite the fact that increasing optical degradation of the GOME scan mirror is observed since 2000 [Tanzi et al., 2001]. For comparison the time series of the TOMS V8 - Lauder differences are also shown. In general, TOMS V8 tends to underestimate ozone during winter/spring thus showing a distinct seasonal cycle in the differences to ground data.

Separating the validation into comparisons with Dobsons and Brewers at the same location and over an
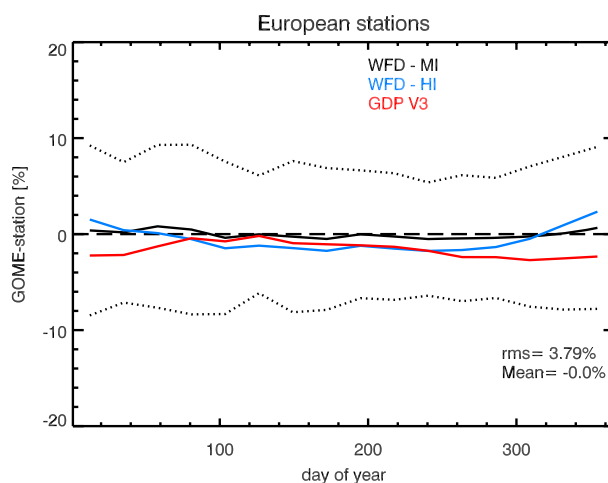
European stations

Figure 13: *Comparison of WFDOAS (black and blue) and V3 GOME total ozone (red) with 9 western European stations at mid-latitudes as a function of the day of year (1996-1999). WFD-MI stands for the retrieval using mid-latitude ozone profile shapes (black, default retrieval) and WFD-HI using high-latitude profile shape (blue, testing the profile shape effect) from the TOMS V7 profile climatology [Wellemeyer et al., 1997]. Black dotted lines are the 2σ scatter of the differences (WFD-MI). Similar results (only shifted according to season) are observed when comparing with SH mid-latitude stations.*

extended period is quite instructive. Such separate comparisons have been carried out with data from Hradec-Kralove (50°N) and Hohenpeissenberg (48°N). Shown are here only the results from Hradec-Kralove as depicted in Fig. 16. The top two panels show the validation with direct sun Brewer and Dobson measurements, respectively. Generally, the agreement is better with the Brewer measurements than with the Dobson. The differences between Dobson and Brewer daily averages from the same day are shown in the bottom panel of Fig. 16. They have a distinct seasonal signature varying from -3% (winter) to 0% (summer) as discussed in Vanicek [1998].
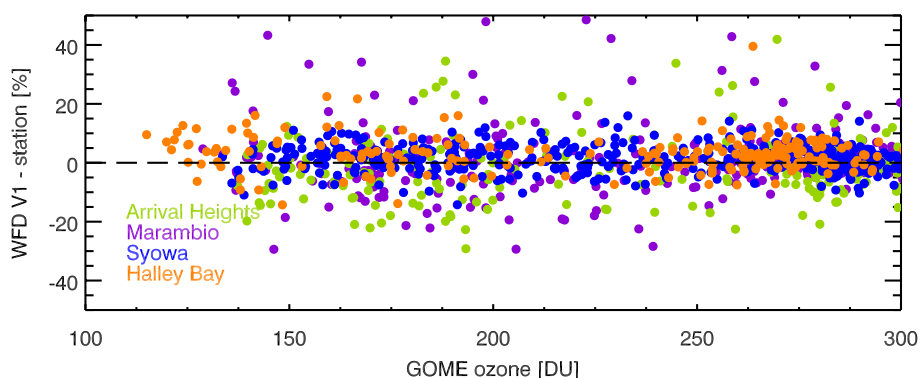
Figure 14: *Comparison of WFDOAS with four SH polar stations (all Dobsons) as a function of retrieved GOME total ozone.*
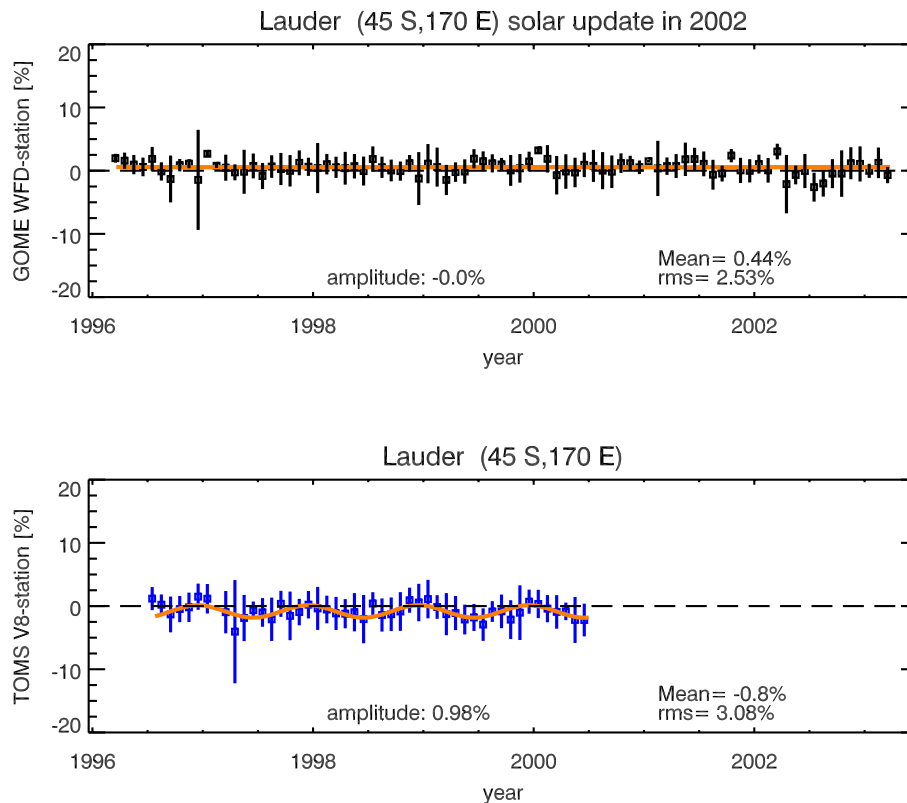
Figure 15: *Monthly mean differences between satellite and Lauder Dobson data. Top panel: WFDOAS, bottom panel: TOMS V8 (until 2000). Orange curves are the results from fitting a sine time series with an annual period to the daily data. After 2000 EP-TOMS suffers from optical degradation effects and results are not shown for the later years.*

The agreement between WFDOAS and Dobson significantly improves if the proper stratospheric ozone temperature is applied in the Dobson and Brewer retrieval. From ozone sonde ascents at Hohenpeissenberg from the same day an ozone profile weighted stratospheric temperature was derived that lead to an average increase of +3 DU in the Brewer and up to +8 DU in the Dobson retrieval during winter [Vanicek et al., 2003]. Taking these corrections into account the WFDOAS comparison particularly with the Hradec-Kralove Dobson improved considerably with no seasonal cycle signature left in the observed differences.

Global validation of GOME WFDOAS with ground-based data shows excellent agreement to within the current uncertainty of ground instrumentation. In the polar region and at high solar zenith angles the new algorithm shows a positive bias, like in the earlier retrieval versions and TOMS retrieval, that needs further investigations in understanding its causes.
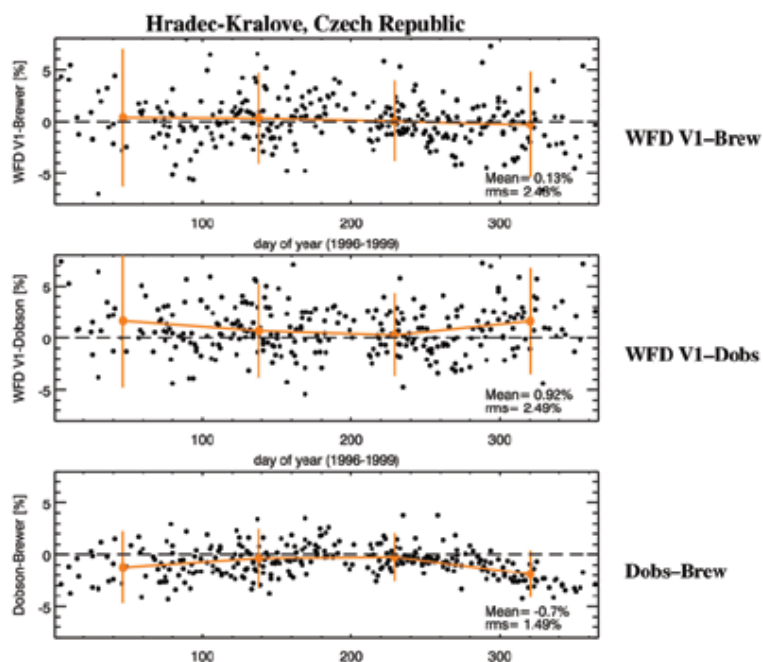
Figure 16: *Differences between WFDOAS and two ground instruments at Hradec-Kralove (50°N). Top: Difference between WFDOAS and Brewer. Middle: between WFDOAS and Dobson. Bottom: Daily difference between Dobson and Brewer. Orange points are the three month average and bars represents 2σ scatter. From Weber et al. [2005]*

3.4.5   Conclusion

A novel type of total ozone retrieval algorithm, called weighting function DOAS, has been developed [Weber et al., 2005, Coldewey-Egbers et al., 2005]. An important element of the new retrieval scheme was the incorporation of other relevant geophysical parameters directly derived from GOME spectral measurements such as cloud parameters and the effective albedo. Another important improvement in the ozone retrieval comes form properly treating the ozone filling-in as part of the Ring effect. This algorithm is attractive for application to SCIAMACHY and future instruments like OMI and GOME2. Bracher et al. [2005] reports on first application of the WFDOAS algorithm to SCIAMACHY data and SCIAMACHY results indicate excellent agreement with GOME.

3.5 Separation of tropospheric and stratospheric columns of minor absorbers

3.5.1 Various methods

The retrieved total columns of minor absorbers such as NO_2 and BrO from nadir sounder like GOME and SCIAMACHY contain information from both troposphere (below about 12 km) and stratosphere (above 12 km). For specific investigations and application, there is considerable interest in separating the tropospheric and stratospheric contribution to the total column [Burrows et al., 1999]. During the last decade global maps of tropospheric absorbers from GOME have been regularly provided for several minor trace gases and they provided important insight into tropospheric chemistry [Richter et al., 1998a,b, Eisinger and Burrows, 1998, Richter and Burrows, 2002, Richter et al., 2002]. Nitrogen dioxide is a trace gas that has large amounts in both troposphere (in boundary layer and under polluted conditions) and stratosphere. For both tropospheric and stratospheric studies the partial columns from the unwanted atmospheric layer is perturbing the quantitative assessment. It is therefore desirable to separate both contributions as best as possible. This project focused on the improvement to derive stratospheric column amounts for NO_2.

For separation of NO_2 total columns into tropospheric and stratospheric columns, following procedures can be applied. Some of these methods are valid for other minor trace gases as well.

- **Reference sector method.** It is assumed that most of the regions on the globe have negligible tropospheric amounts and the total column then equals the stratospheric columns. Those regions are used to identify references for stratospheric column amounts that can be subtracted from any total columns to obtain the tropospheric amount. This would be a valid approach if stratospheric amounts are constant at least for a given latitude. In case of NO_2 this is not the case since stratospheric variability is significant.

- **Ocean as reference.** This method is an extension of the reference sector method. Here, oceanic regions and, possibly, other regions as well that are characterized by lack of NO_2 emission are selected as reference. Particular disadvantage is that one has to interpolate over large distances across continents. In addition, elevated NO_2 emissions can be transported across oceans that further limit the accuracy of the column separation by this method.

- **Cloud cover.** When the satellite observes scenes full cloud cover, most of the tropospheric column is hidden from the satellite view and the partial column above the cloud then represents the stratospheric column. Assuming that stratospheric variability is small as it is approximately the case in the tropics, one may estimate tropospheric columns in cloud free scenes by subtracting stratospheric columns above near-by clouds from the observed total column [Ziemke et al., 1998]. In a further refinement, on can attempt to use the variation in derived cloud heights to quantify trace gas amounts in specific layers near the tropopause. The latter method is known as the cloud slicing method [Ziemke et al., 2001]. One has to keep in mind that high clouds that extend up to the tropopause are only found in tropical convective systems, so that this method of separation only reliably works in the tropics. GOME has a ground coverage of about $320{\times}40$ km^2 that is fairly large as compared to other satellite instruments such as TOMS ($50{\times}50$ km^2) that limits the probability of full cloud cover occurrences. For SCIAMACHY with an improved spatial resolution down to $30{\times}30$km^2, this method is more suitable.
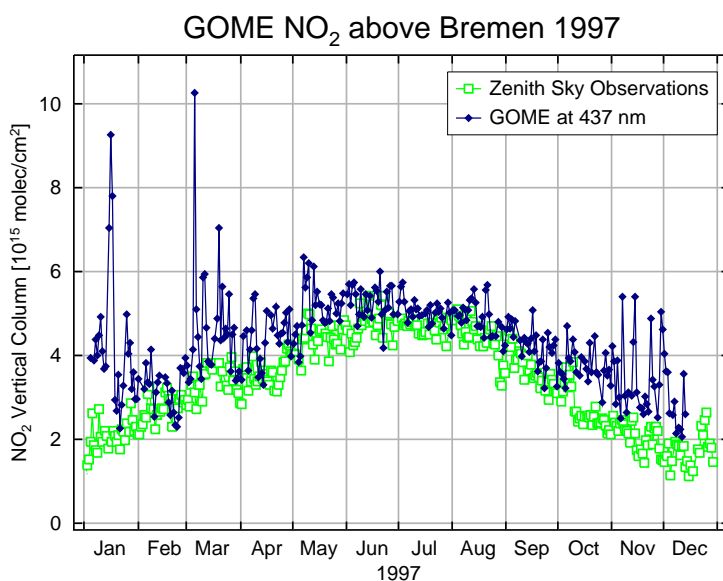
Figure 17: *GOME NO$_2$ vertical columns derived from the 425–450 nm fitting window. Shown is the mean of all GOME measurements within a 500 km radius around Bremen (53°N, 9°E). The red lines shows the zenith-sky results from the ground. The daily mean values have been obtained by linearly interpolating between the morning and evening mean to time of GOME overpass. Generally the agreement is quite good except for selected days where GOME shows elevated tropospheric contribution form pollution events in Northern Germany.*

- **Wavelength selection.** At different wavelengths the sensitivity to certain atmospheric layers differ. For instance, at short wavelengths Rayleigh scattering increases so that most photons comes form upper atmospheric layers. At longer wavelengths in the visible the contribution of photons and absorption near the ground is higher particularly when the surface albedo is elevated. Using retrievals form different wavelength regions can therefore be helpful by differentiating between contributions from different atmospheric layers [Richter and Burrows, 2002].

The wavelength method is particularly suitable for NO$_2$ due to non-negligible absorption both in the UV and visible spectral range. This method can be demonstrated by comparing GOME retrievals at different wavelengths with ground-based zenith sky observations from Bremen.

The Bremen UV/visible spectrometer works similar like the GOME instrument, but it has a very limited sensitivity to the troposphere. Zenith sky observations are usually done during sunrise and sunset, where the stratospheric contribution is enhanced due to the longer path through the stratosphere. In addition a specific corrections to remove the tropospheric column has been applied by accounting for the (atmospheric) temperature sensitivity of the NO$_2$ cross-section in the DOAS retrieval. For each day a morning and evening value for the Bremen observations are obtained but GOME observations are mostly around late morning to noon. Within a radius of 500 km around Bremen all GOME observations form the same day have been averaged. The morning and evening results from the Bremen spectrometer have been linearly interpolated to the GOME overpass time. A comparison for the year 1997 is shown in Fig. 17. In this figure the GOME retrievals at 425-450 nm are compared. Generally, the GOME values are higher than the ground data. For selected days the satellite observations strongly exceeds the Bre-
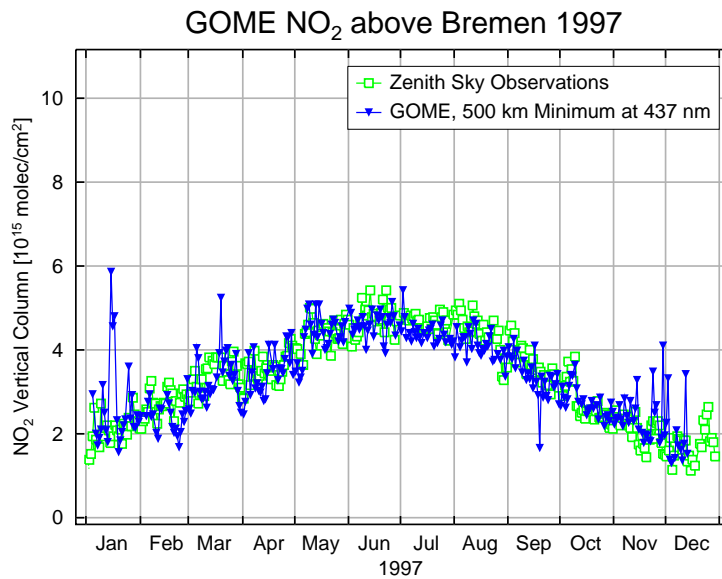
Figure 18: *The same as Fig. 17 except that only minimum GOME NO$_2$ total columns within a radius of 500 km around Bremen are shown. Better agreement to ground measurements are evident, but for some days elevated GOME NO$_2$ amounts are still observed.*
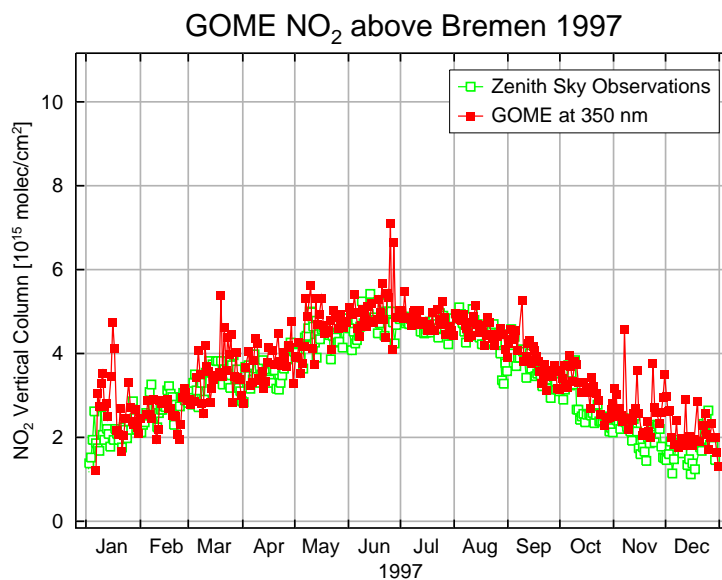
Figure 19: *The same as Fig. 17 except GOME retrievals that are derived from the fitting window 345–359 nm. The use of UV wavelengths in the GOME retrieval has reduced the tropospheric contributions to the total column resulting in better agreement to ground data. Due to the weaker NO$_2$ absorption in the UV as compared to the visible, the scatter in the GOME data has increased.*

men measurements. This supports the notion that at visible wavelengths GOME observes tropospheric pollutions that are not seen in the ground data.

Comparing only minimum GOME NO_2 for each day within a 500 km radius around Bremen somewhat improves the comparison as shown in Fig. 18. However, for some days the satellite observations still show elevated tropospheric amounts that are not present in the measurements from the ground. Nevertheless, a significant improvement has been achieved by using minimum total columns, but the spatial resolution (radius of 500 km) in the satellite measurements has been reduced.

Figure 19 now shows a comparison of GOME retrievals in the UV fitting window (345–359 nm) using the same selection criterion as shown in Fig. 17. This fitting windows is usually used for the GOME BrO retrieval and the comparison of the UV NO_2 total column between GOME and the ground has significantly improved. It has been demonstrated that stratospheric retrieval of nitrogen dioxide can be improved using UV wavelengths for the DOAS retrievals.

3.5.2   Conclusion

Several methods are available that permit the derivation of tropospheric and stratospheric contributions to the retrieved total column. This is important for the interpretation of minor trace gases, its sources and distribution in various atmospheric layers. These methods can be applied in general to any minor absorber and ozone and are attractive for other space instruments like SCIAMACHY, OMI, and GOME-2, as well. With regard to the wavelength method described here further work is needed to show that this method is suitable for global application. Differencing retrievals from different fitting windows may help to improve tropospheric corrections to the observed stratospheric columns.

3.6 Dynamical and chemical contribution to mid- to high latitude ozone

3.6.1 Decadal ozone variability

The main contributions of decadal ozone variability are changes in solar flux, changes in ozone depleting substances and changes in stratospheric circulation patterns. In order to study long term changes in ozone, it is necessary to separate influence of various dynamical and chemical processes as well as processes that act both on short and long term time scales. Short term processes are Quasi-biennial Oscillation (QBO), El Nino/Southern Oscillation index (ENSO or SOI) [SPARC, 1998, WMO, 2003], variation in tropopause heights [Weber et al., 2002, see for instance], volcanic eruptions and tropospheric driven planetary wave activity which controls ozone transport into high latitudes as part of the residual circulation [Fusco and Salby, 1999].

The zonally averaged transport circulation in the wintertime stratosphere consists of a single mean meridional cell in each hemisphere with a rising branch in the tropics, poleward flow at mid latitudes and downward mass transport at higher latitudes. This circulation is driven by momentum deposited by breaking waves [Andrews et al., 1987]. Waves propagate from the troposphere to the stratosphere, break at critical levels and decelerate the mean zonal wind. Coriolis force and pressure gradient are not in equilibrium anymore and poleward motion sets in. The mass transport from the equator to the pole leads to adiabatic heating at high latitudes and drives stratospheric temperatures away from radiative equilibrium [Newman et al., 2001]. Diabatic cooling sets in and leads to subsidence of air masses. This residual circulation also tightly controls the wintertime ozone buildup at high latitudes [Fusco and Salby, 1999, Randel and Stolarski, 2002]. The ability of waves to propagate vertically is dependent on the zonal mean flow and, therefore, wave activity is strongest in the winter of the respective hemisphere. This explains the strong increase in ozone during winter as shown in Fig. 20. This signal of the strength of the residual circulation is even preserved until next autumn as evident in the color coding of the curves for NH ozone in Fig. 20 and as shown in the scatter plot of Fig. 21 [Fioletov and Shepherd, 2003].

3.6.2 Dynamical control of ozone transport and chemistry

The magnitude of momentum transport via planetary waves from the troposphere into the stratosphere is represented by the Eliassen-Palm (EP) flux vector. It is believed that this momentum and energy transfer are caused by a combination of orographic waves and thermal forces driven by sea surface temperatures, for instance. The eddy heat flux $\overline{v'T'}$ which is directly proportional to the vertical component of EP flux vector is found to be a very attractive proxy to determine the magnitude of the wave activity [Fusco and Salby, 1999, Newman et al., 2001, Weber et al., 2003]. Various other dynamical proxies such as Arctic Oscillation (AO) or North Atlantic Oscillation (NAO) index, polar jet strength index, tropopause height, polar stratospheric cloud (PSC) volume, 50 hPa temperature which are well correlated with each other and in turn, are controlled by wave activity [Randel and Cobb, 1994, Baldwin and Dunkerton, 1999, Chipperfield and Jones, 1999, Fusco and Salby, 1999, Randel and Stolarski, 2002, Salby and Callaghan, 2002, Plumb and Semeniuk, 2003, Steinbrecht et al., 2003].

Ozone is affected by the planetary wave driving in several ways: a stronger residual circulation means that more ozone is transported from its source region at the equator to higher latitudes, that meridional mixing is stronger, more ozone is transported downwards at high latitudes, where it is photochemically
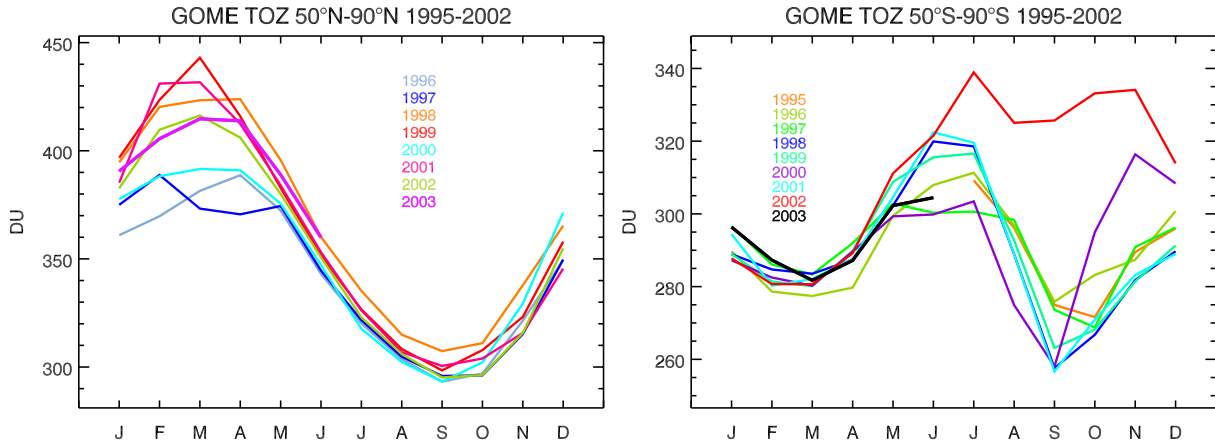
Figure 20: *Annual course of GOME total ozone between 1995 and 1996 for both hemispheres (50°-90° latitudes).*
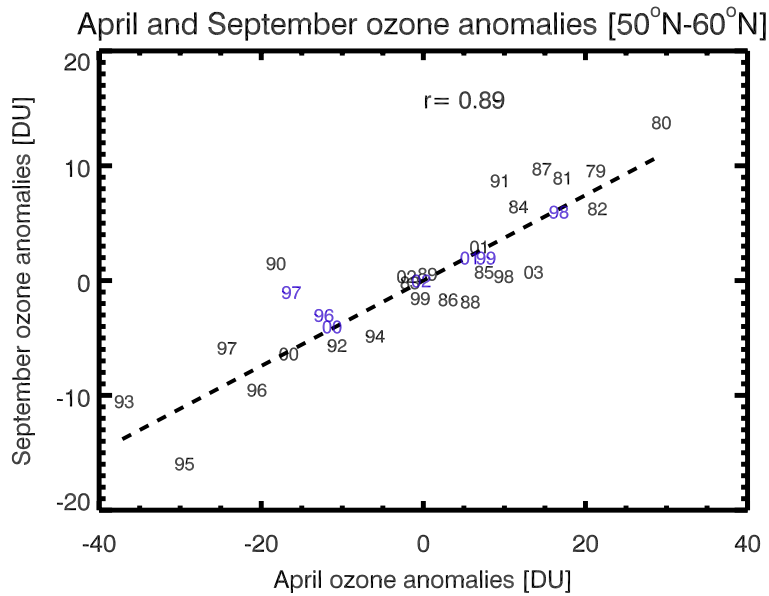
Figure 21: *Correlation between September and April total ozone anomaly for latitude band 50°N-60°N from SBUV V8 data (1979-2003, black) and GOME (1995-2003, blue).*
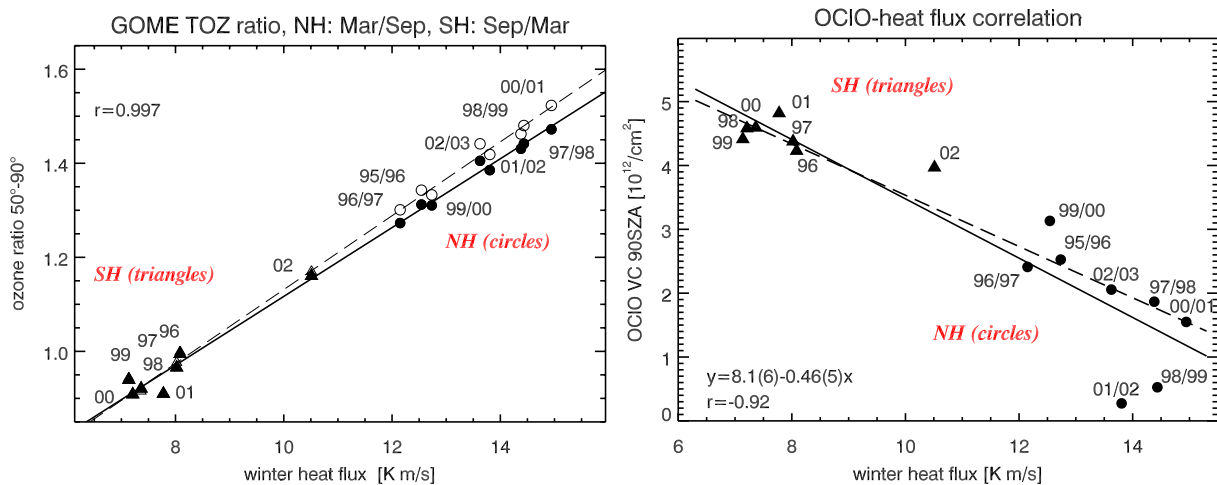
Figure 22: *Winter ozone gain (March over September ratio in NH and September over March ratio in SH) polewards of 50° (left) and mean maximum GOME OClO vertical column (right) as a function of winter eddy heat flux. Daily maximum OClO vertical column observed at 90° solar zenith angle were averaged over the entire SH and NH winter/spring season to obtain the OClO mean. Solid line is a linear fit through the data. For OClO the dashed line shows the least absolute deviation (LAD) fit. OClO outlier data for Arctic winter 1998/99 and 2001/02 may be due to sampling problems since polar vortex area was very small during those winter. The dashed line in the ozone plot is the fit through the GOME V3 operational data (light circles). Solid circles are the new WFDOAS total ozone results from Coldewey-Egbers et al. [2005]. Update from Weber et al. [2003]*

more stable, stratospheric temperatures rise, and less ozone is chemically depleted via heterogeneous reactions. Figure 22 shows the winter ozone gain (September over March ratio in NH and September over March ratio in SH) as a function of the mean hemispheric eddy heat flux during winter [Weber et al., 2003]. Also shown are the accumulated maximum OClO vertical columns from GOME as a function of the mean edddy heat flux as derived from ERA-40 [Simmons and Gibson, 2000]. OClO is a measure of chlorine activation from heterogeneous reaction on polar stratospheric clouds that are responsible for the fast chemical depletion inside the polar vortex, particularly in SH winter/spring [Wagner et al., 2001]. In the southern hemisphere the chemical depletion by heterogeneous chemistry (Antarctic ozone hole) clearly outweighs the gain in transport (winter gain ratio smaller than one) while during northern hemispheric winters the ozone gain by transport clearly exceeds polar ozone loss as shown in Figs. 20 and 22. The SH polar spring 2002 is an exception where a net increase in polar ozone from fall to spring has been observed. This winter/spring has been termed the Antarctic ozone hole anomaly and will be discussed in the next section. In general inter-annual ozone variability is larger in NH winter/spring than in SH.

Changes in ozone transport and chemistry are dynamically controlled and strongly coupled. This is important with regard to future evolution of the ozone layer in a changing climate that may alter the stratospheric circulation pattern under conditions of decreasing stratospheric chlorine loading (as a consequence of the Montreal Protocol phasing out ozone depleting substances) [Schnadt et al., 2002, Butchart and Scaife, 2001].

Weber et al.   *Universität Bremen*
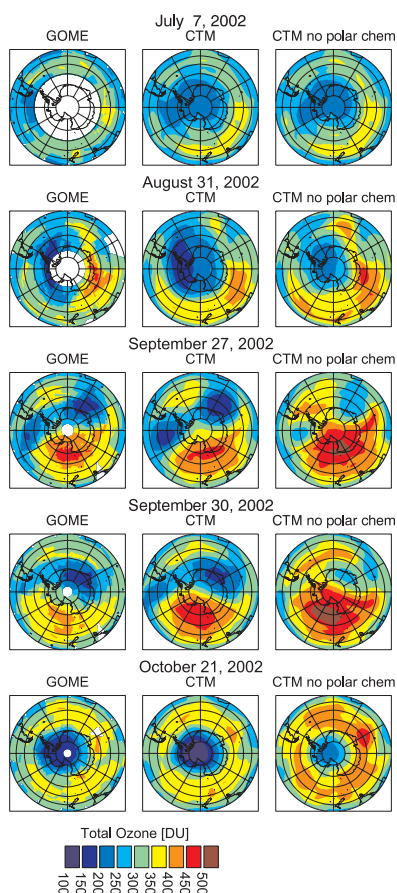
Figure 23: *SH total ozone from GOME (left) and chemistry-transport model calculation using UKMO met analysis winds and temperature with heterogeneous chemistry included (middle) and without (right) for selected days in 2002 (top to bottom). From Sinnhuber et al. [2003].*

3.6.3   Antarctic ozone hole anomaly in 2002

Figures 20 and 22 show that polar ozone during Antarctic winter was unusually high. One of the major reason for this unusual event is the exceptionally high eddy heat flux that were observed throughout the winter. A particular high surge in eddy heat flux was observed on September 21 and 22, 2002 that was followed by the first major stratospheric warming to be observed in the southern hemisphere. This resulted in a split of the polar vortex within a few days [Weber et al., 2003, Sinnhuber et al., 2003]. One part of the vortex weakened and polar airmasses were mixed into mid-latitudes while the other part moved back to the pole and remained stable until the final warming at the end of October.

Chemistry-transport model results with and without heterogeneous chemistry on PSCs are shown with GOME results for selected days during Antarctic spring 2002 in Fig. 23. From the ozone-eddy heat flux correlation (Fig. 22) it seems that this SH winter appears to be an intermediate case between typical Antarctic winters (with low planetary wave activity and low ozone) and typical cold Arctic winters (like 1995/96, 1996/97, and 1999/2000). The CTM results show that polar ozone loss (heterogeneous chem-
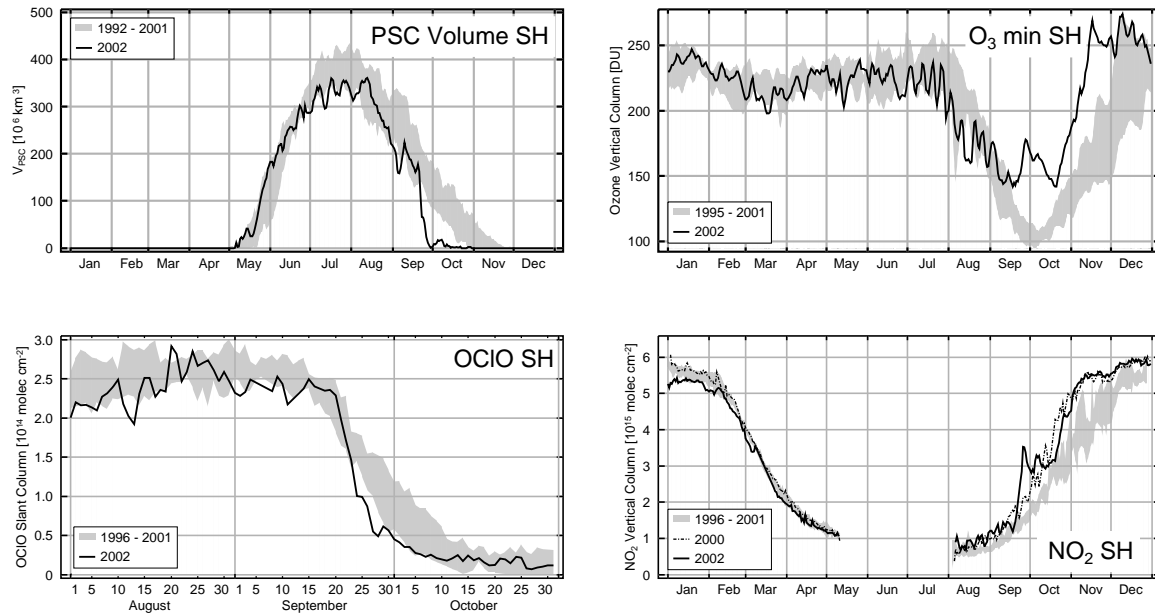
Figure 24: *Top left: Daily PSC volume at extra-tropical latitudes as approximated by the temperature region between 100 hPa and 4 hPa, where stratospheric temperature according to UKMO meteorological analysis was below T_{NAT}, a threshold temperature for possible existence of polar stratospheric clouds. Top right: Daily minimum GOME total ozone observed polewards of $50°S$. Bottom left: OClO slant columns observed by GOME in the southern hemisphere. The values given are the average of all measurements taken between $89°$ and $91°$ solar zenith angle where the potential vorticity on the 495 K potential temperature level (about 19 km altitude) was above 36 PVU. Bottom right: Annual cycle of GOME NO_2 vertical columns averaged over $70°$ - $80°$ south. In the southern hemisphere, no data are available for May, June and July as the solar zenith angle at the time of GOME overpass is larger than the threshold value of $92°$. In all panels shadings indicate the range observed before 2000 (for NO2 year 2001 has also been excluded) and solid lines represents data from 2002. From Richter et al. [2005]*

ical loss) was comparable to other SH winter. This seems to be supported by the observed accumulated winter OClO for 2002 that was only slightly below the values for other SH winters as shown in Fig. 22.

This Antarctic spring was characterized by a perturbed chemistry that not only affected ozone but also other trace gases such as NO_2 and OClO. Figure 24 shows OClO, minimum total ozone, and NO_2 from GOME in 2002 in comparison to earlier years. During the SH major warming event at the end of September elevated NO_2 columns were observed. The OClO data show that chlorine deactivation was faster than in other years, but values (and also the PSC volume from UKMO met analyses) were in the normal range of other years [Richter et al., 2005].

3.6.4   Conclusion

Eight years of GOME trace gas data are very valuable for scientific case studies such as dynamical and chemical contribution to ozone changes as well as for investigation of the perturbed chemistry during Antarctic winter 2002. Continuation of observations will be provided by SCIAMACHY (launched in

2002), OMI (launched in 2004) and GOME-2 (launch in 2006). In a paper by von Savigny et al. [2005] SCIAMACHY trace gas observations from limb measurements have complemented GOME observations of the Antarctic ozone hole anomaly. Multiple data sets are very important to follow decadal changes in ozone and other trace gases in a changing climate.

References

D. G. Andrews, J. R. Holton, and C. B. Leovy. *Middle Atmosphere Dynamics*. Academic Press, 1987.

M. P. Baldwin and T. J. Dunkerton. Propagation of the Arctic Oscillation from the stratosphere to the troposphere. *J. Geophys.Res.*, 104,30937–30946, 1999.

H. Bovensmann, J. P. Burrows, M. Buchwitz, J. Frerick, S. Noel, V. V. Rozanov, K. V. Chance, and A. H. P. Goede. SCIAMACHY - Mission objectives and measurement modes. *J. Atmos. Sci.*, 56, 125–150, 1999.

A. Bracher, M. Weber, K. Bramstedt, M. Coldewey-Egbers, L. N. Lamsal, and J. Burrows. Global satellite validation of SCIAMACHY O_3 columns with GOME WFDOAS. *Atmos. Chem. Phys. Discuss.*, 5,795–813, 2005.

M. Buchwitz. *Strahlungstransport- und Inversionsalgorithmen zur Ableitung atmosphärischer Spurengasinformationen aus Erdfernerkundungsmessungen in Nadirgeometrie im ultravioletten bis nahinfraroten Spektralbereich am Beispiel SCIAMACHY*. PhD thesis, Institut für Umweltphysik, Universität Bremen, 2000.

M. Buchwitz, V.V. Rozanov, and J.P. Burrows. A near-infrared optimized DOAS method for the fast global retrieval of atmospheric CH_4, CO, CO_2, H_2O, and N_2O total column amounts from SCIAMACHY Envisat-1 nadir radiances. *J. Geophys. Res.*, 105,15,231–15,245, 2000.

J.P. Burrows, M. Weber, M. Buchwitz V. V.Rozanov, A. Ladstädter-Weissenmayer A. Richter, R. de Beek, K. Bramstedt R. Hoogen, K.-U. Eichmann, M. Eisinger, and D. Perner. The Global Ozone Monitoring Experiment (GOME): Mission concept and first scientific results. *J. Atmos. Sci.*, 56,151–175, 1999.

N. Butchart and A. A. Scaife. Removal of chlorofluorocarbons by increased mass exchange between the stratosphere and troposphere in a changing climate. *Nature*, 410,799–802, 2001.

M. P. Chipperfield and R. L. Jones. Relative influences of atmospheric chemistry and transport on Arctic ozone trends. *Nature*, 400,551–554, 1999.

M. Coldewey-Egbers, M. Weber, M. Buchwitz, and J.P. Burrows. Application of a modified DOAS method for total ozone retrieval from GOME data at high polar latitudes. *Adv. Space Res.*, 34,749–753, 2004.

M. Coldewey-Egbers, M. Weber, L. N. Lamsal, R. de Beek, M. Buchwitz, and J. P. Burrows. Total ozone retrieval from GOME UV spectral data using the weighting function DOAS approach. *Atmos. Chem. Phys.*, 5,5015–5025, 2005.

R. de Beek, R. Hoogen, V.V. Rozanov, and J.P. Burrows. Ozone profile retrieval from GOME satellite data I: Algorithm description. In T.-D. Guyenne and D. Danesy, editors, *Space at the Service of our Environment*, volume II of *ESA SP-414*, pages 749–754, ESTEC, Noordwijk, The Netherlands, May 1997. European Space Agency, ESA Publications Division. 3rd ERS Scientific Symposium, 17-21 March 1997, Florence, Italy.

R. de Beek, V.V. Rozanov, and J.P. Burrows. Ozone total columns and vertical profiles from the Global Ozone Monitoring Experiment (GOME): Theory. In J.A. Pyle, N.R.P. Harris, and G.T. Amanatidis, editors, *Polar Stratospheric Ozone - Proceedings of the 3rd European Workshop*, volume 56 of *Air Pollution Research Report*, pages 833–838, Luxembourg, 1996. BMBF, European Commission. 18.–22. September 1995, Schliersee, Germany.

R. de Beek, M. Vountas, V. V. Rozanov, A. Richter, and J. P. Burrows. The Ring effect in the cloudy atmosphere. *Geophys. Res. Lett.*, 28,721–724, 2001.

R. de Beek, M. Weber, V.V. Rozanov, A. Rozanov, A. Richter, and J.P. Burrows. Trace gas column retrieval - An error study for GOME-2. *Adv. Space Res.*, 34,727–733, 2004.

M. Eisinger and J.P. Burrows. Tropospheric sulfur dioxide observed by the ERS-2 GOME instrument. *Geophys. Res. Lett.*, 25,4177–4180, 1998.

V. E. Fioletov and T. G. Shepherd. Seasonal persistence of midlatitude total ozone anomalies. *Geophys. Res. Lett*, 30, 2003.

P. Fortuin and H. Kelder. An ozone climatology based on ozonesonde and satellite measurements. *J. Geophys. Res.*, 103,31,709–31,734, 1998.

A. C. Fusco and M. L. Salby. Interannual variations of total ozone and their relationship to variations of planetary wave activity. *J. Climate*, 12,1619–1629, 1999.

GDP V3 VALREPORT. ERS-2 GOME GDP 3.0 implementation and delta validation report. Technical Note ERSE-DTEX-EOAD-TN-02-0006, Issue 1.0, ed. J.-C. Lambert, November 2002, see also: http://earth.esrin.esa.it/pub/ESA_DOC/GOME/gdp3/gdp3.htm, 2002.

J. R. Herman and E. A. Celarier. Earth surface reflectivity climatology at 340-380 nm from TOMS data. *J. Geophys. Res.*, **102**(D23),28003–28011, 1997.

R. Hoogen, V. V. Rozanov, K. Bramstedt, K.-U. Eichmann, M. Weber, and J. P. Burrows. O_3 profiles from GOME satellite data - I: Comparison with ozonesonde measurements. *Phys. Chem. Earth*, 24, 447–452, 1999a.

R. Hoogen, V. V. Rozanov, and J. P. Burrows. Ozone profiles from GOME satellite data: Algorithm description and first validation. *J. Geophys. Res.*, 104,8263–8280, 1999b.

J. Joiner and P. K. Barthia. Rotational Raman scattering (Ring effect) in satellite backscatter ultraviolet measurements. *Appl. Opt.*, 34,4513–4525, 1995.

J. Joiner and P. K. Bhartia. The determination of cloud pressures from rotational Raman scattering in satellite backscatter ultraviolet measurements. *J. Geophys. Res.*, 100,23019–23026, 1995.

R. B. A. Koelemeijer, J. F. de Haan, and P. Stammes. A database of spectral surface reflectivity in the range 335–772 nm derived from 5.5 years of GOME observations. *J. Geophys. Res.*, 108, doi:10.1029/2002JD002429, 2003.

R. B. A. Koelemeijer, P. Stammes, J. W. Hovenier, and J. F. de Haan. A fast method for retrieval of cloud parameters using oxygen A-band measurements from the Global Ozone Monitoring Experiment. *J. Geophys. Res.*, 106,3475–3496, 2001.

L.N. Lamsal, M. Weber, S. Tellmann, and J. P. Burrows. Ozone column classified climatology of ozone and temperature profiles based on ozonesonde and satellite data. *J. Geophys. Res.*, 109,D20304, doi:10.1029/2004JD004680, 2004.

Y.J. Meijer, R.J. van der A, R.F. van Oss, D.P.J. Swart, and H.M. Kelder. Global Ozone Monitoring Experiment ozone profile characterization using interpretation tools and lidar measurements for inter-comparison. *J. Geophys. Res.*, 108,doi:10.1029/2003JD003498, 2003.

P. A. Newman, E.R. Nash, and J.E. Rosenfield. What controls the temperature of the arctic stratosphere during the spring? *J. Geophys. Res.*, 106,19999–20010, 2001.

R. A. Plumb and A. Semeniuk. Downward migration of extratropical zonal wind anomalies. *J. Geophys. Res.*, 108, 2003.

W. J. Randel and J. B. Cobb. Coherent variations of monthly mean column ozone and lower stratospheric temperature. *J. Geophys. Res.*, 99,5433–5447, 1994.

W. J. Randel and R. S. Stolarski. Changes in column ozone correlated with EP flux. *J. Meteor. Soc. Jpn.*, 80,849–862, 2002.

A. Richter, F. Wittrock A., A. Ladstätter-Weissenmayer, and J.P. Burrows. Gome measurements of stratospheric and tropospheric bro. *Adv. Space Res.*, 29,1667–1672, 2002.

A. Richter and J.P. Burrows. Retrieval of tropospheric NO2 from GOME measurements. *Adv. Space Res.*, 29,1673–1683, 2002.

A. Richter, M. Eisinger, F. Wittrock, and J.P. Burrows. Measurements of halogen oxides by GOME. *Earth Observ. Quart.*, 58,19–20, 1998a.

A. Richter, F. Wittrock, M. Eisinger, and J.P. Burrows. Gome observations of tropospheric BrO in northern hemispheric spring and summer 1997. *Geophys. Res. Lett.*, 25,2683–2686, 1998b.

A. Richter, F. Wittrock, M. Weber, S. Beirle, S. Kühl, U. Platt, T. Wagner, W. Wilms-Grabe, and J.P. Burrows. GOME observations of stratospheric trace gas distributions during the splitting vortex event in the Antarctic winter 2002 Part I: Measurements. *J. Atmos. Sci.*, 62,778–785, 2005.

V. V. Rozanov, T. Kurosu, and J. P. Burrows. Retrieval of atmospheric constituents in the UV/visible: A new analytical approach to calculating weighting functions. *J. Quant. Spectrosc. Rad. Transfer*, 60, 277–299, 1998.

M.L. Salby and P.E. Callaghan. Interannual changes of the stratospheric circulation: relationship to ozone and tropospheric structure. *J. Climate*, 15,3673–3685, 2002.

C. Schnadt, M. Dameris, M. Ponater, R. Hein, V. Grewe, and B. Steil. Interaction of atmospheric chemistry and climate and its impact on stratospheric ozone. *Clim. Dyn.*, 18,501–518, 2002.

A. J. Simmons and J. K. Gibson. The ERA-40 project plan. Technical report, ECMWF, Reading UK, 2000. ERA-40 Project Report Series no. 1.

B.-M. Sinnhuber, M. Weber, A. Amankwah, and J.P. Burrows. Total ozone during the unusual Antarctic winter of 2002. *Geophys. Res. Lett.*, 30,1850, doi:10.1029/2002GL016798, 2003.

SPARC. *Assessment of Trends in the vertical distribution of ozone, in WMO Ozone Research and Monitoring Project Report No. 34*, pages 3413–3418. World Climate Research Programme, WCRP-113,WMO/TD-No.1043, 1998.

J. Staehelin, J. Kerr, R. Evans, and K. Vanicek. Comparison of total ozone measurements of Dobson and Brewer spectrophotometers and recommended transfer functions. Technical report, WMO, 2003. World Meteorological Organization Global Atmosphere Watch (WMO-GAW) Report 149.

W. Steinbrecht, B. Hassler, H. Claude, and P. Winkler anR. Stolarski. Global distribution of total ozone and lower stratospheric temperature variations. *Atmos. Chem. Phys.*, 3,3411–3449, 2003.

C. P. Tanzi, R. Snel, O. Hasekamp, and I. Aben. Degradation of UV earth albedo observations by GOME. In *ERS-ENVISAT Symposium, Gothenburg, 16-20 October 2000*, 2001. ESA Special Publication SP-461 (CD-ROM).

S. Tellmann. *Ozonvertikalverteilungen aus UV/Vis-Nadirspektren des Satelliteninstrumentes GOME: Optimierung und Sensitivitätsstudien zur Nutzung der achtjährigen Messreihen*. PhD thesis, Universität Bremen, 2005.

S. Tellmann, V.V. Rozanov, M. Weber, and J.P. Burrows. Improvements in the tropical ozone profile retrieval from GOME UV/vis nadir spectra. *Adv. Space Res.*, 34,739–743, 2004.

K. Vanicek. Differences between Dobson and Brewer observations of total ozone at Hradec-Kralove. In R.D. Bojkov and G. Visconti, editors, *Atmospheric Ozone, Proc. Quadr. Ozone Symp.*, pages 81–84. Edigrafital S.p.A.-S.Atto (TE), 1998.

K. Vanicek, M. Stanek, and M. Dubrovsky. Evaluation of Dobson and Brewer total ozone observations from Hradec Kralove Czech Republic, 1961–2002. Technical report, Czech Hydrometeorological Institute, 2003. EU Project CANDIDOZ EVK2-2001-00024, Working Group WG-1.

C. von Savigny, A. Rozanov, H. Bovensmann, K.-U. Eichmann, S. Noel, V. V. Rozanov, B.-M. Sinnhuber, M. Weber, J. P. Burrows, and J. Kaiser. The ozone hole break-up in September 2002 as seen by SCIAMACHY on ENVISAT. *J. Atmos. Sci.*, 62,721–734, 2005.

M. Vountas, V.V. Rozanov, and J.P. Burrows. Ring effect: Impact of rotational Raman scattering on radiative transfer in earth's atmosphere. *J. Quant. Spectrosc. Radiat. Transfer*, 60(6),943–961, 1998.

T. Wagner, C. Leue, K. Pfeilsticker, and U. Platt. Monitoring of the stratospheric chlorine activation by GOME OClO measurements in the austral and boreal winters 1995 through 1999. *J. Geophys. Res.*, 106,4971–4996, 2001.

M. Weber, S. Dhomse, F. Wittrock, A. Richter, B.-M. Sinnhuber, and J. P. Burrows. Dynamical control of NH and SH winter/spring total ozone from GOME observations in 1995-2002. *Geophys. Res. Lett.*, 30,doi:10.1029/2002GL016799, 2003.

M. Weber, K.-U. Eichmann, F. Wittrock, K. Bramstedt, L. Hild, A. Richter, J.P. Burrows, , and R. Müller. The cold arctic winter 1995/96 as observed by the Global Ozone Monitoring Experiment GOME and HALOE: Tropospheric wave activity and chemical ozone loss. *Quart. J. Roy. Meteor. Soc.*, 128,1293–1319, 2002.

M. Weber, L. N. Lamsal, M. Coldewey-Egbers, K. Bramstedt, and J. P. Burrows. Pole-to-pole validation of GOME WFDOAS total ozone with groundbased data. *Atmos. Chem. Phys.*, 5,1341–1355, 2005.

C. G. Wellemeyer, S. L. Taylor, C. J. Seftor, R. D. McPeters, and P. K. Bhartia. A correction for the Total Ozone Mapping Spectrometer profile shape errors at high latitude. *J. Geophys. Res.*, 102,9029–9038, 1997.

WMO. Scientific assessment of ozone depletion: 2002. Global Ozone Research and Monitoring Project Report 47, World Meteorological Organizatio, Geneva, 2003. URL `http://www.wmo.ch/web/arep/ozone. html`.

J.R. Ziemke, S. Chandra, and P.K. Barthia. Two new methods for deriving tropospheric column from TOMS measurements: The assimilated UARS MLS/HALOE and convective-cloud differential techniques. *J. Geophys. Res.*, 103,22,115–22,127, 1998.

J.R. Ziemke, S. Chandra, and P.K. Barthia. Cloud slicing: A new technique to derive uper tropospheric ozone from satellite measurements. *J. Geophys. Res.*, 106,9853–9867, 2001.

4 Publikationen von GOMSTRAT

A. Bracher, M. Weber, K. Bramstedt, M. Coldewey-Egbers, L. N. Lamsal, and J. Burrows, Global satellite validation of SCIAMACHY O$_3$ columns with GOME WFDOAS, *Atmos. Chem. Phys. Discuss.*, 5, 795–813, 2005

K. Bramstedt, J. Gleason, D. Loyola, W. Thomas, A. Bracher, M. Weber, and J. P. Burrows, Comparison of total ozone from the satellite instruments GOME and TOMS with measurements from the Dobson network 1996-2000, 2002, *Atmos. Chem. Phys.*, 3, 1409-1419, 2003.

M. Coldewey-Egbers, M. Weber, M. Buchwitz, and J.P. Burrows, Application of a modified DOAS method for total ozone retrieval from GOME data at high polar latitudes, *Adv. Space Res.*, 34, 749-753, 2004.

M. Coldewey-Egbers, M. Weber, L. N. Lamsal, R. de Beek, M. Buchwitz, and J. P. Burrows, A total ozone algorithm for backscatter UV using the weighting function DOAS approach, *Atmos. Chem. Phys.*, 5, 1015-1025, 2005.

A. Darmawan, Improved Dynamical Climatology of Ozone for Use in Optimal Estimation Retrieval, MSc Thesis, University of Bremen, 2002.

L. N. Lamsal, M. Weber, S. Tellmann, and J. P. Burrows, Ozone column classified climatology of ozone and temperature profiles based on ozonesonde and satellite data, *J. Geophys. Res.*, 09, D20304, doi:10.1029/2004JD004680, 2004.

A. Richter, F. Wittrock, M. Weber, S. Beirle, S. Kühl, U. Platt, T. Wagner, W. Wilms-Grabe, and J.P. Burrows, GOME observations of stratospheric trace gas distributions during the splitting vortex event in the Antarctic winter 2002 Part I: Measurements, *J. Atmos. Sci.*, 62, 778-785, 2005.

B.-M. Sinnhuber, M. Weber, A. Amankwah, and J.P. Burrows, Total ozone during the unusual Antarctic winter of 2002, 2003, *Geophys. Res. Lett.*, 30, 1850, doi:10.1029/2002GL016798, 2003.

S. Tellmann, V.V. Rozanov, M. Weber, and J.P. Burrows, Improvements in the tropical ozone profile retrieval from GOME UV/vis nadir spectra, *Adv. Space Res.*, 34, 739-743, 2004.

S. Tellmann, Ozonvertikalverteilungen aus UV/Vis-Nadirspektren des Satelliteninstrumentes GOME: Optimierung und Sensitivitätsstudien zur Nutzung der achtjährigen Messreihen, PhD. Thesis, University of Bremen, 2005.

M. Weber, S. Dhomse, F. Wittrock, A. Richter, B.-M. Sinnhuber, and J.P. Burrows, Dynamical control of NH and SH winter/spring total ozone from GOME observations in 1995–2002, 2003, *Geophys. Res. Lett.*, 30, 1853, doi:10.1029/2002GL016799, 2003.

M. Weber, L. N. Lamsal, M. Coldewey-Egbers, K. Bramstedt, and J. P. Burrows, Pole-to-pole validation of GOME WFDOAS total ozone with groundbased data, *Atmos. Chem. Phys.*, 5, 1341-1355, 2005.